The University of Southern Mississippi

The Aquila Digital Community

Spring 5-2008

Evaluating Vascular Plant Composition and Species Richness on Horn Island, Mississippi, Using Passive and Active Remote Sensing in Conjunction with Ground Based Measurements

Kelly Lynn Lucas
University of Southern Mississippi

The University of Southern Mississippi

EVALUATING VASCULAR PLANT COMPOSITION AND SPECIES RICHNESS

ON HORN ISLAND, MISSISSIPPI, USING PASSIVE AND ACTIVE REMOTE

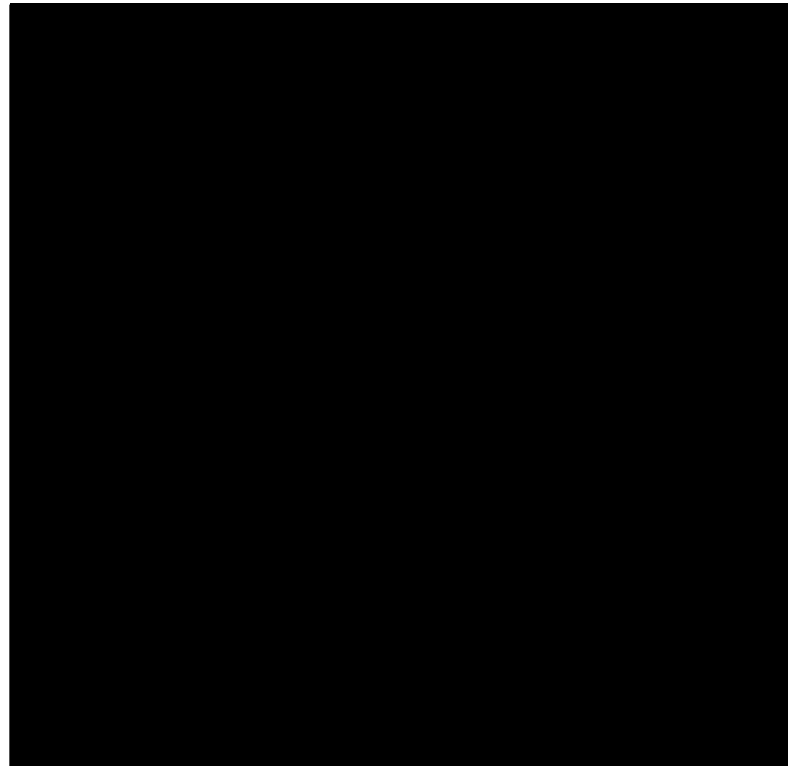SENSING IN CONJUNCTION WITH GROUND BASED MEASUREMENTS

by

Kelly Lynn Lucas

A Dissertation
Submitted to the Graduate Studies Office
of The University of Southern Mississippi
in Partial Fulfillment of the Requirements
for the Degree of Doctor of Philosophy

Approved:

May 2008

The University of Southern Mississippi

EVALUATING VASCULAR PLANT COMPOSITION AND SPECIES RICHNESS

ON HORN ISLAND, MISSISSIPPI, USING PASSIVE AND ACTIVE REMOTE

SENSING IN CONJUNCTION WITH GROUND BASED MEASUREMENTS

by

Kelly Lynn Lucas

Abstract of a Dissertation
Submitted to the Graduate Studies Offices
of The University of Southern Mississippi
in Partial Fulfillment of the Requirements
for the Degree of Doctoral Philosophy

May 2008

ABSTRACT

EVALUATING VASCULAR PLANT COMPOSITION AND SPECIES RICHNESS

ON HORN ISLAND, MISSISSIPPI, USING PASSIVE AND ACTIVE REMOTE

SENSING IN CONJUNCTION WITH GROUND BASED MEASUREMENTS

by Kelly Lynn Lucas

May 2008

Barrier island vegetation is subjected to chronic abiotic stressors combined with

periodic storm events that favor species adapted to harsh environments. These islands are

the first landforms to be affected by changes in coastal subsidence and sea-level rise.

Evaluating changes in vegetation is important for understanding the impact of global

climate change on coastal environments.

This study assesses vegetation composition and plant species richness on Horn

Island, Mississippi using ground data in conjunction with remotely sensed spectral and

LIDAR data. The goals of this research are to: 1) classify and map vegetation

composition on Horn Island using hyperspectral and LIDAR data, 2) evaluate changes in

vegetation composition through comparison with a vegetation study and classification

map from 1979, 3) determine the extent to which vascular plant species richness might be

estimated using remotely sensed spectral reflectance indices and spatial variability within

these indices, and 4) utilize the vertical distribution of airborne multiple-return LIDAR

data to evaluate vascular plant species richness.

The vegetation composition of habitat-types on Horn Island can be identified by

indicator species that are consistent both over time and among other barrier islands.

Additionally, combining airborne hyperspectral and LIDAR data improved the overall

classification accuracy of habitats. Although only broad comparisons in vegetation changes could be made between this study and previous maps, these changes were linked with geomorphological changes.

In simple linear regressions, various reflectance- and LIDAR-indices correlated significantly ($p \leq 0.05$) with richness when habitat-types were considered individually. Regressions of richness with indices derived from within-transect means or spatial variability in reflectance, reflectance band ratios, as well as vertical distribution descriptors and height percentiles from LIDAR data produced estimation errors of 0.4-2.5 species per transect. Best-fit indices from hyperspectral data indicate spectral bands in the near- and mid-infrared spectra are most important in the estimation of plant species richness while LIDAR indices indicate the importance of vegetation height and structural complexity in estimating plant species richness.

The capability of utilizing remotely sensed data to classify vegetation composition and estimate species richness provides a promising means of assessing and monitoring vegetation on barrier islands.

ACKNOWLEDGEMENTS

TABLE OF CONTENTS

            Introduction
            Methods
            Results and Discussion
            Conclusions

            Introduction
            Methods
            Results
            Discussion and Conclusions

            Introduction
            Methods
            Results
            Discussion and Conclusions

LIST OF TABLES

Table

LIST OF ILLUSTRATIONS

CHAPTER I

INTRODUCTION

Along the Atlantic and Gulf coasts of the United States, barrier islands constitute

approximately 85% of the open-ocean shoreline (Stauble, 1989). Barrier islands protect

the mainland coast from higher energy waves of the open ocean (Snyder & Boss, 2002),

and they foster the creation of productive estuaries, coastal wetlands, and aquatic

environments (Godfrey, 1976) as well as supply food and shelter for resident and

migratory animals. Existing at the land-sea interface these islands are constantly

changing in response to waves, wind, current, sediment supply, storms, rising sea-level,

and coastal subsidence, potentially making them the important indicators of global

climate change (Pilkey, 2003). Barrier island conditions foster plant species that are

highly adapted to environmental stressors such as salt spray, saltwater, and freshwater

flooding, drought, burial by sand, and poor soil nutrients (Oosting, 1954; Shao, Shugart,

& Hayden, 1996). Expectations are that sea-level rise will accelerate (Holgate &

Woodworth, 2004; Zhang, Douglas, & Leatherman, 2004), tropical storms will increase

in frequency and severity (Hayden & Hayden, 2003), and human populations in coastal

zones will expand rapidly (US Commission on Ocean Policy (USCOP), 2004). All these

factors require efficient methods of assessing and monitoring vegetation and biodiversity

on barrier islands to better understand the impact of global climate change on coastal

environments.

Vegetation assessment through the use of remote sensing is becoming a powerful

approach in defining diversity patterns, monitoring change, and aiding in conservation

efforts (Mooney & Chapin, 1994; Rey-Benayas & Pope, 1995). Generally, such methods

rely on the direct detection of organisms or community types or on more indirect

relationships of biodiversity with habitat class along with climate or primary productivity estimates (Turner et al., 2003). Although most current techniques for using remote sensing to assess biodiversity address regional to global scales, land use and conservation decisions are generally made at mesoscales (1-100 km^2) (Kareiva 1993; O'Neil et al., 1997; Stoms, 1994). Thus, the development of techniques for assessing biodiversity at these scales should prove directly beneficial in natural resource management and conservation. Plant species richness, the number of species in a given location, is an essential characteristic of ecosystems (Chapin et al., 2000; Hooper & Vitousek, 1997; Tilman et al., 1997) and its assessment via remote sensing provides a useful measure of biodiversity (Stoms & Estes, 1993).

In Mississippi, Horn Island presents an ideal setting for the development of remote sensing methods in coastal biodiversity assessment. Horn Island (30° 13'N, 88° 40'W) was placed under the jurisdiction of the Gulf Islands National Seashore, US National Park Service, in 1971. Designated as a Wilderness Area in the National Wilderness Preservation System, it is one of more than 50 barrier islands that border the northern Gulf of Mexico and contains a variety of habitats including beach dunes, swales, lagoons, ponds, fresh and saltwater marshes, and maritime forest. The island is located 18 km seaward of the Mississippi mainland shore. Prior to Hurricane Katrina (August 29, 2005), the island was approximately 22 km long (E-W), a maximum of 1 km wide (N-S) and included approximately 1300 ha of land area above mean high-tide level. Previous surveys of vascular plants on Horn Island identified 260 species, occurring in five habitats: beach dunes, stable dunes, woodland, marsh, and meadow (Eleuterius, 1979).

This research looks to address species richness and habitat composition as well as evaluate and develop passive and active remote sensing techniques for estimating plant species richness on Horn Island. The following objectives will be explored in chapters II-IV:

Chapter II: Classification of plant communities and historical comparison

The main objectives of this chapter are to: 1) classify and map the vegetation on the Horn Island using hyperspectral data, LIDAR data, and combined hyperspectral and LIDAR data, 2) describe the composition of plant communities within the island, 3) evaluate plant species richness from randomly selected island locations, and 4) compare the vegetation map produced as part of this study with a vegetation map prepared in 1979 (Eleuterius, 1979).

Chapter III: The use of passive remote sensing to assess plant species richness

The goal of this portion of the study is to utilize hyperspectral data acquired from an airborne platform at high spatial resolution (HyMap) to directly assess vascular plant species richness on Horn Island, Mississippi. Primary objectives are to: 1) determine correlations of plant species richness at randomly-selected island locations with relatively simple reflectance indices (band ratios and spectral derivatives), 2) determine correlations of spatial variability in these indices with richness, and 3) evaluate the consistency with which a particular index may correlate strongly with richness among island habitats.

Chapter IV: The use of airborne LIDAR to assess plant species richness

The goal of this study is to exploit the vertical distribution of airborne multiple-return LIDAR to directly evaluate vascular plant species richness on Horn Island. Primary objectives are to: 1) determine correlations of plant species richness at randomly-

selected island locations with vertical distribution descriptors such as mean, standard

deviation, and range, and 2) determine correlations of plant species richness with

vegetation height expressed at each 10th percentile above the minimum elevation as well

as ratios of percentiles.

CHAPTER II

CLASSIFYING AND COMPARING VEGETATION ON HORN ISLAND,

MISSISSIPPI, USING AIRBORNE HYPERSPECTRAL IMAGING, MUTIPLE-

RETURN LIDAR AND HISTORICAL MAPS

Introduction

Along the Atlantic and Gulf of Mexico coasts of the United States, barrier islands

constitute approximately 85% of the open-ocean shoreline (Stauble, 1989). They protect

mainland shores from the high energy waves of the open ocean (Snyder & Boss, 2002;

Stive & Hammer-Klose, 2004), foster the creation of biologically productive estuaries,

coastal wetlands, and aquatic environments (Godfrey, 1976), and supply food and shelter

for resident and migratory animals. Existing at the land-sea interface, these islands

change continually in response to waves, wind, currents, sediment supply, storms, rising

sea-level, and coastal subsidence, potentially defining them as important indicators of

global climate change (Pilkey, 2003). The barrier island environment favors plant species

that are highly adapted to environmental stressors such as salt spray, saltwater and

freshwater flooding, drought, burial by sand, and low soil nutrient content (Lee &

Ignaciuk, 1985; Oosting, 1954; Shao et al., 1996). Expectations are that sea-level rise will

accelerate (Holgate & Woodworth, 2004; Zhang, Douglas, & Leatherman, 2004), tropical

storms will increase in frequency and severity (Hayden & Hayden, 2003), and human

populations in coastal zones will expand rapidly (USCOP, 2004). All these factors

require efficient methods of assessing and monitoring vegetaion on barrier islands to

better understand the impact of global climate change on coastal environments.

Vegetation maps not only provide a visual interpretation of the vegetation distribution but also help in evaluating and monitoring natural and anthropogenic effects on the landscape. To be successful, resource management plans need to include baseline maps of land cover (Geevan, 1995). Remotely sensed data such as aerial photography, videography, airborne, and satellite spectral sensors, RADAR(radio detection and ranging), and LIDAR(light detection and ranging) provide primary data sources that can be used to assess and monitor vegetation (Griffith, Stehman, Sohn, & Loveland, 2000; Turner et al, 2003). Classifying and mapping vegetation in coastal communities has been accomplished using aerial photography (Eleuterius, 1979; Dorp, Boot , & van der Maarel 1985), airborne, and satellite spectral sensors (Bachmann, et al., 2002; Lucas, Shanmugam, & Barnsely, 2002; Ramsey, Nelson, Echols, & Sapkota, 2002; Wang, Traber, Milstead, & Stevens, 2007) and combined spectral and LIDAR elevation data (Lee & Shan, 2003). Analysis of sequential vegetation maps over years have also been used to evaluate and monitor changes in vegetation patterns and relate the patterns to changes in ecological processes or management activities in coastal landscapes (Dorp et al., 1985; Janssen, 2004; Acosta, Carranza, & Izzi, 2005).

This study begins by describing and quantifying the vegetation composition on Horn Island, Mississippi and comparing the vegetation patterns with other Gulf of Mexico barrier islands as well as previous studies of Horn Island. In addition, this study classifies and maps the vegetation on Horn Island using: 1) high resolution (3 m) hyperspectral data, 2) LIDAR data, and 3) combined hyperspectral and LIDAR data. Supervised classification results for each data type are compared and evaluated using overall accuracy as well as errors of commission and omission from confusion matrix

statistics. This classification is compared with a vegetation classification map from 1979 in order to examine changes in habitat composition on Horn Island over time.

Methods

Study Area

Located 18 km seaward of the Mississippi mainland shore, Horn Island (30° 13'N, 88° 40'W) (Fig. 1) was placed under the jurisdiction of the Gulf Islands National Seashore, U.S. National Park Service, in 1971 and is designated as a Wilderness Area in the National Wilderness Preservation System. The island is part of a 105 km long barrier island chain spanning westward from the mouth of Mobile Bay, Alabama to Cat Island, Mississippi, forming the southern boundary of the Mississippi Sound. Horn Island formed 3000 to 4000 years ago (Otvos, 1970) and the holocene sand platform is about 12 m thick (Otvos, 1979). The sediment is composed of quartz sand, heavy minerals, and shell (Cipriani & Stone, 2001). Horn is one of more than 50 barrier islands that border the northern Gulf of Mexico and contains a variety of habitat types. These include beach dunes, swales, lagoons, ponds, fresh and saltwater marshes, and maritime forest. All data for this study were acquired prior to Hurricane Katrina (August 29, 2005) when the island was approximately 22 km long (E-W), a maximum of 1 km wide (N-S), and included approximately 1300 ha (1.30 km^2) of land area above mean high-tide level. The climate is humid subtropical with an average air temperature of 12° C in winter and 27° C in summer. Average annual precipitation is 140 cm with a peak in July due mainly to thunderstorms.
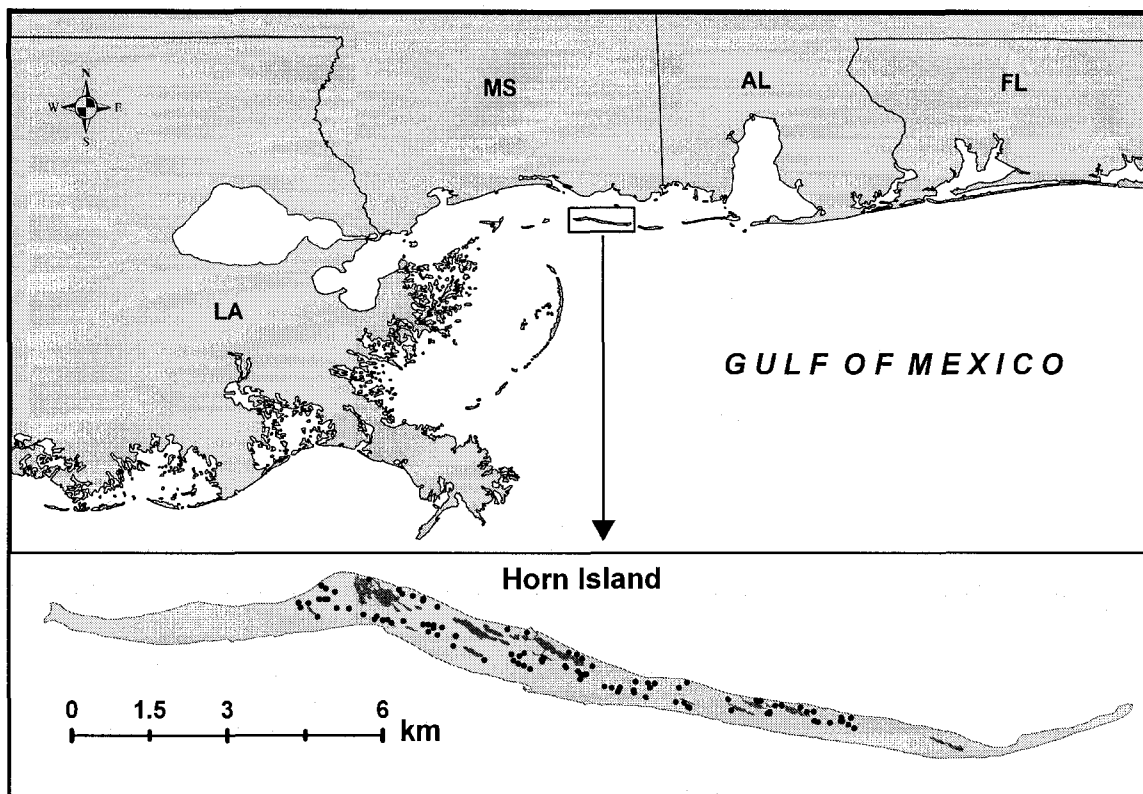
Fig. 1. Map of the northern Gulf of Mexico and Horn Island, Mississippi. The expanded

map of Horn indicates the random placement of 100, 15-m line transects established for

ground-sampling of plant species richness. Darker-gray areas represent inland ponds or

lagoons. No transects were established on the eastern and western ends of the island

because these areas were subject to vegetation change during the interval between image

acquisition and ground sampling

Image Data Acquisition and Pre-processing

s*pectral data.* Hyperspectral imagery of Horn Island was acquired on October, 15, 2003 by the HyMap airborne imaging system (HyVista Corporation, NSW, Australia). The HyMap sensor employed a rotating scan mirror that constructed an image line-by-line as the aircraft flew forward. Four 32-element detector arrays provided a 126-band data cube that spanned the 450 to 2500 nm spectral range for each pixel in a 512-pixel swath. Full-width-at-half-maximum (FWHM) bandwidths were approximately 15 nm. The above-ground flight altitude of 1400 m produced a 3 m ground sample distance (GSD). An on-board GPS provided geographic latitude and longitude information for each pixel (WGS 1984, UTM Zone 16N) stored in an Input Geometry (IGM) file.

HyVista calibrated the data to apparent reflectance using HyCorr, a program similar to the ATmospheric REMoval program (ATREM) (Gao, Heidebrecht, & Goetz, 1992) to reduce the affects of atmospheric absorption and scattering mechanisms. Bands centered at 456, 858, 873, 1390, 1406, 1420, 1952, and 2490 nm were deleted due to strong atmospheric interference, detector overlap or insensitivity resulting in a 118-channel data cube. To further refine the scaling to reflectance, spectral reflectance for five areas of dry beach sand devoid of vegetation was measured in-situ on Horn Island using a field-portable spectroradiometer (model ASD-FS, Analytical Spectral Devices, Boulder, CO). Comparison of in-situ reflectance with reflectance output by HyCorr for the same sand areas showed similar spectra differing by approximately 10 percent on average. Thus, a scaling factor for each spectral band was determined by dividing in-situ reflectance by image (HyCorr) reflectance representing the same areas. The HyCorr-

output data were multiplied by the scaling factor to yield an improved calibration of image data to percentage reflectance.

LIDAR data. The Compact Hydrographic Airborne Rapid Total Survey (CHARTS) system was flown over Horn Island in April, 2004 by the Joint Airborne LIDAR Bathymetry Technical Center of Expertise. Laser pulses were emitted with a wavelength of 1064 nm at a 10 kHz repetition rate. The aircraft flew at an above ground altitude of 400 m, creating less than 1 m spot density with first and last returns recorded for each laser pulse. Multiple passes were made over each flight line to increase the coverage of returns. The on board GPS system provides latitude and longitude of each return in North American Datum (NAD) of 1983 and vertical return data in NADV of 1988 UTM Zone 16N. The LIDAR data were supplied by the NOAA Coastal Services Center as two binary raster files with 3 m pixels. One file contained the minimum return (elevation) for each 3 m pixel and the other contained the maximum return. The maximum return is considered the first return received by the sensor and represents a return from the canopy (Lefsky, Cohen, Parker, & Harding, 2002). The map projection for each raster file was converted to WGS 1984 using rigorous mapping method to transform every pixel in the image (ENVI v. 4.2).

fusion. Before fusing the LIDAR and HyMap data, known ground control targets were analyzed for positional accuracy in both images. The accuracy was within 1 pixel (3m) in the horizontal; therefore, no further refinement was necessary and the images were considered co-registered. Both data sets were then fused with one another resulting in a 120 band image consisting of the 118 spectral bands and the LIDAR minimum and maximum returns.

historical imagery and maps. A vegetation map of Horn Island prepared as part of a phytosociological study conducted from 1976 to 1978 was digitized at 600dpi, converted to a raster with 1m pixel resolution and geo-referenced (UTM Zone 16N, WGS 1984) to 1975 aerial photography acquired by the United States Geological Survey using island features. The vegetation maps were prepared using aerial photography and ground vegetation surveys to delineate plant community types (Eleuterius, 1979). The map is considered by the National Park Service as being highly accurate at the time of publication. However, microhabitats or micro-plant communities ranging from a few square meters to one hectare occurring within larger predominate communities were not mapped (Eleuterius, 1979). For ease of comparison the pixels were re-sampled to 3 m spatial resolution to match the HyMap and LIDAR data.

Ground Vegetation Sampling

Vascular plant species richness for this study was sampled at 100, 15 m line transects that were established at random locations (Fig. 1). Approximately 6 months to one year elapsed between the onset of ground vegetation sampling and image acquisition in 2003 for HyMap and 2004 for LIDAR. During this time, a fire on the western end of the island (2003) and storm overwash of the extreme eastern end in Hurricane Ivan (2004) potentially altered species composition. Thus, the western and eastern ends of the island were not sampled (Fig. 1). Also, beach dunes were eliminated from study as the only habitat-type in which significant changes in vegetative cover might occur during a storm-free year. Otherwise, there was no indication of significant change in species composition on the remainder of the island. Horn Island vegetation is dominated by evergreen species. Other than senescence in annual plants, the vegetation was vigorous

and not exposed to drought between image acquisitions and the completion of ground sampling. Transect sampling began in November, 2004 and continued through May, 2005. Spot-checks in April and May, 2005, of transects sampled during the autumn and winter months verified that species composition had remained consistent through the end of the sampling period.

Random points on the island derived from the georectified HyMap image (ENVI v. 4.2) were imported to a Trimble GPS receiver (model GeoXT, Trimble Software, Sunnyvale, CA) for use in establishing field transect locations (Fig. 1). Once a point was located in the field it became the center of a 15 m line transect. Habitat-type at transect center was defined according to the Horn Island vegetation classification system previously established by Eleuterius (1979). Transect azimuth was directed toward the nearest habitat transition (e.g., woodland to meadow) to capture species richness in transition zones as well as in the clearly-defined habitat-types. In transition zones, species that are characteristic of a given habitat-type are found mixed with those of an adjacent, different habitat-type. The randomization of transect location resulted in the following number of transects per habitat-type: marsh (10), meadow (18), stable dune (39), woodland (6), and transition zone (27). Sampling was limited to the imaginary vertical plane which contained the transect line. Only species which intersected the plane were counted. Species richness for each transect was calculated as the total number of unique species located on each transect and species richness of each habitat was calculated as total number of unique species found in each habitat-type. Regardless of its abundance, a species was counted only once per transect. Additional data recorded for each transect included percent bare soil (percentage of total transect length which

intersected sky-exposed bare soil), percent cover for species intersecting the transect plane, GPS locations of transect end points and photographs taken from each end point. For each habitat including the transition zone, frequency was determined by calculating the percentage of transects on which a species occurred. Vegetation cover was determined for each habitat by subtracting percent bare soil from 100. In addition, frequency and cover was determined from all 100 transects. In accordance with the permit granted by the National Park Service, no destructive sampling took place, no specimens were removed from the island and no permanent markers were placed on the island.

Classification

Maximum likelihood (ML) was selected as the supervised classification method because it is widely accepted and generally provides the greatest accuracy among various supervised classification procedures (Jensen, 2005). It computes the probability that a certain pixel belongs to one of a pre-defined number of classes, taking into account the variability in each region of interest (ROI) and assuming that training data statistics in each band for each class are normally distributed. The pixel is then assigned to the class to which it most likely belongs. ML classification was performed on HyMap data, LIDAR data, and the fused HyMap and LIDAR data. Classification accuracy was determined by error matrix and the K_{hat} coefficient of agreement (Jensen, 2005). This produced values for errors of omission and errors of commission. K_{hat} accounts for errors of omission and commission and indicates the degree of classification accuracy with respect to ground reference data.

To reduce the data volume of HyMap for ML classification a discriminate function analysis (DFA) was employed. Regions of interest were created from the GPS locations recorded for transects along with GPS locations for known habitat-types. The spectral information for marsh, meadow, stable dune, woodland, beach dune, and shoreline or intertidal beach was imported into SPSS (SPSS Inc, Chicago, IL) for DFA. Transition zone was not included in the classification. In order to build the discrimination model, individual wavelengths were chosen by a stepwise selection process based on calculations of P-values resulting from multivariate partial- F test ($p \leq$ 0.05). Results of the DFA indicate that only 8 HyMap spectral bands are necessary to separate the classes with the greatest accuracy. Therefore, bands with wavelengths located at 470, 484, 530, 573, 661, 691, 950, and 980 nm were included in the ML classification of the HyMap data. For each ROI representing a habitat class, 90 pixels were randomly chosen for utilization in the ML classification and 75 pixels were reserved for accuracy assessment. ML classification of the two band LIDAR image as well as the combined 8 HyMap spectral bands and two LIDAR bands, was performed using the same randomly selected ROIs for each habitat. A 110 ha portion on the north side of the island was not covered by the LIDAR; therefore ROIs used in both the classification and accuracy assessment were not from this area.

Results and Discussion

Species richness and habitats

A total of 260 vascular plant species were reported previously for Horn Island by counting species found in 45, 256m^2 circular plots examined three times over the course of two-years, as well as species found on the island as part of a flora survey (Eleuterius, 1979). Analyzing only the plot data from Eleuterius (1979), 154 total species were recorded from all habitats. Eliminating species located only in beach dunes resulted in 136 total species recorded in the circular plots. Only 69 species were found in this study (Table 1); however, the line-transect approach differed from earlier sampling methods. The vascular plant species recorded from the 100 transects sampled during this study represented three divisions of plant life: Pteriodophyta, Coniferophyta and Magnoliophyta. The species were divided into 26 families with Poaceae, Asteraceae, and Cyperaceae containing 25%, 10%, and 7%, respectively, of the total species. The number of species per transect ranged from 0 to 12. The most frequently found species in this study was yaupon holly (*Ilex vomitoria*) closely followed by torpedo grass (*Panicum repens*).

Table 1. Field data of total number of species for each habitat and for all habitats combined along with mean species richness and cover with one standard deviation shown in parentheses. Ground elevation was calculated from the minimum return in the LIDAR data. The 100 transect locations resulted in the following number of transects per habitat-type: marsh (10), meadow (18), stable dune (39), woodland (6), and transition zone (27) Only 90 transects were covered by the LIDAR flight lines and the number of represented transects are shown in brackets after the standard deviation which is shown in parentheses.

Habitat	Total Species	Species Richness	Cover (%)	Elevation (m)
Marsh	16	4.0 (1.4)	98 (6.0)	0.7 (0.2) [10]
Meadow	38	6.8 (3.0)	63 (30)	1.1 (0.2) [16]
Stable Dune	34	4.4 (1.8)	58 (27)	1.7 (0.8) [37]
Transition Zone	44	6.8 (2.1)	72 (22)	1.0 (0.3) [22]
Woodland	12	5.0 (2.2)	88 (15)	1.0 (0.1) [5]
All Habitats Combined	69	5.5 (2.4)	68 (30)	1.3 (0.6) [90]

marsh. At the lowest elevations, marsh habitat exhibited flooded to near-saturated soils with almost 100 percent cover by vegetation (Table 1). Richness averaged four species per transect and was dominated by saltmeadow cordgrass *(Spartina patens)* and black needle rush (*Juncus roemerianus*) (Table 2). These two species also occurred with the greatest frequency in the 1979 phytosociological study of Horn Island, with saltmeadow cordgrass occurring in 100% of the plots and black needle rush occurring in 78% of the plots (Eleuterius, 1979). These species have also been recorded at Ship Island (Miller & Jones, 1967) located 9 km to the west of Horn Island as well as Cat Island (Penfound & O'Neill, 1934) located about 30 km west of Horn Island and on Perdido Key, Florida (Looney, Gibson, Blyth, & Cousens, 1993). In addition, marsh habitat exhibited minimal seasonal variation on Perdido Key with the dominant species *Juncus roemerianus* used as an indicator species in three out of four seasons (Gibson & Looney, 1992).

meadow. Meadows are located in swales and flat areas between dunes that are often found at slightly higher elevations than marsh. In swales, depth to the freshwater table has been found to play a key role in vegetation composition (Hayden, Santos, Shao, & Kochel, 1995; Rheinhardt & Faser, 2001). The soils vary from a wet peat covered by vegetation to exposed often dryer sandy areas. Meadows averaged seven species per transect and vegetation cover was 63 percent (Table 1). Meadows were characterized primarily by herbaceous vegetation dominated by torpedo grass (*Panicum repens*) and goldentop (*Euthamia leptocephala*) (Table 2). The most abundant meadow species on Horn Island reported by Eleuterius (1979) were southern umbrella-sedge (*Fuirena scirpoidea)* (89%) and torpedo grass (88%). Reports of plant abundance in swales from

other Gulf of Mexico barrier islands vary. Whereas torpedo grass was found to be the most third abundant species in swales on Cat Island (Penfound & O'Neill, 1934) following LeConte's flatsedge (*Cyperus lecontei*) and seaside pennywort (*Hydrocotyle bonariensis*), swales were dominated by saltmeadow cordgrass and yaupon holly on Perdido Key (Gibson & Looney, 1992). Torpedo grass was listed as abundant on Ship Island but no habitat was given (Miller & Jones, 1967).

stable dunes. Stable dunes are fixed dunes that support sparse vegetation cover by perennial shrubs and trees. Others have referred to this type of habitat as wooded dunes (Gibson & Looney, 1992), shrub dunes (Burkhalter, 1987), stabilized dunes (Doing, 1985) or fixed dunes (Moreno-casasola & Espejel, 1986). Stable dunes were found at the highest elevations and included the greatest percentage of bare soil (sand) along with a species richness of four species per transect (Table 1). The dunes were dominated by woody golden rod (*Chrysoma paucifloculosa*) and beach rosemary (*Ceratiola ericoides*) (Table 2). Also, yaupon holly was third most abundant occurring in 41% of the transects. Eleuterius (1979) referred to stable dune habitat as relic dunes and found species frequencies of 100 % for woody golden rod, 79% for rockrose (*Helianthemum arenicola*), and 65% for beach rosemary. Reports from Cat Island indicate that rockrose and woody goldenrod were extremely abundant, but to a lesser degree beach rosemary was a common component of stable dune complexes (Penfound & O'Neill, 1934); however, reports from Ship Island found beach rosemary abundant on stable dunes (Miller & Jones, 1967). Woody goldenrod, beach rosemary, and rockrose were reported as abundant on Dauphin Island the eastern most island in the chain located 22 km to the east of Horn Island (Deramus, 1970).

transition zone. Transition zones occurred where there was a gentle slope producing areas of mixed species of two adjacent but distinct habitat types. Transition zones averaged seven species per transect (Table 1), and were located primarily between meadows and stable dunes and secondarily between marsh and stable dunes. Transition-zone soils were often moist and vegetation cover was approximately 70 percent. This coverage was greater than in meadows and stable dunes but less than in woodlands and marshes. Saltmeadow cordgrass and torpedo grass were the most abundant species (Table 2). These species were followed closely in abundance by yaupon holly and slash pine (*Pinus elliottii*) which occurred with frequencies of 52% each.

woodland. Woodlands were dominated by yaupon holly which occurred in all the woodland transects and slash pine which occurred in all but one transect (Table 2). Additionally, wax myrtle (*Myrica cerifera*) and poison ivy (*Toxicodendron radicans*) occurred with frequencies of 50%. Sand live oak (*Quercus geminata*) occurred as a minor component of woodlands in the eastern central part of the island. Woodlands had high vegetative cover and averaged five species per transect. Woodland habitat was near the same elevation as meadow habitat, but higher than marsh and lower than stable dunes (Table 1). According to Eleuterius (1979), southern umbrella-sedge and wax myrtle appeared with the greatest frequency of 67% in woodland plots. Yaupon holly and slash pine showed a 40% and 59% frequency in same 1979 study (Eleuterius, 1979) with poison ivy occurring in only 18% of the plots. Slash pine was also recorded as abundant in woodlands on Ship Island (Miller & Jones 1969) and Dauphin Island (Deramus, 1970) but only moderately abundant (28%) on Cat Island (Penfound and O'Neill, 1934). Studies of the woodlands of Horn and Cat Islands showed that no species occurred at

frequency of greater than 69% (Eleuterius, 1979; Penfound & O'Neill, 1934). For Horn

Island, 9, 256m^2 woodland plots were studied (Eleuterius, 1979) and for Cat Island

somewhere between 25 and 100, 1m^2 woodland plots were analyzed (Penfound &

O'Neill, 1934). However, the random design of this study resulted in only 6, 15 m line

transects, which may account for the higher frequencies of occurrence. In addition, slash

pine was found as the dominant woodland species on Horn Island in a 1941 study, and

yaupon holly was noted as a common shrub that reached heights of 7 m (Pessin &

Burleigh, 1942).

Table 2. Frequency of the two most prevalent species for each habitat and for all habitats combined.

Habitat	Species	Frequency
Marsh	*Spartina patens*	90
	Juncus roemerianus	80
Meadow	*Panicum repens*	72
	Euthamia leptocephala	61
Stable Dune	*Chrysoma pauciflosculosa*	54
	Ceratiola ericoides	44
Transition Zone	*Spartina patens*	59
	Panicum repens	59
Woodland	*Ilex vomitoria*	100
	Pinus elliottii	83
All Habitats Combined	*Ilex vomitoria*	45
	Panicum repens	42

Classification

The ML classification results indicated that integration of LIDAR and HyMap data improved the overall classification accuracy 20% over classifications of LIDAR or HyMap data alone. The 0.89 kappa coefficient of agreement (K_{hat}) for the combined data indicated strong agreement between the ground truth areas and the derived classifications (Table 3). Overall accuracy was determined by dividing the number of correctly classified pixels by the total number of pixels. Individually, LIDAR and HyMap overall classification accuracies were about equal. However, marsh and meadow habitat were more accurately classified with HyMap having both a greater producer's and user's accuracy and a lower omission and commission error when compared to the LIDAR classification, but stable dune was more accurately classified with LIDAR. (Table 3, Fig 2).

Producer's accuracy measures how well a category can be classified and is calculated by dividing the correctly classified pixels in a category by the total number of reference pixels (75) in the category. In addition, omission error or the number of pixels that were not correctly classified can be determined by subtracting the producer's accuracy from 100 percent. User's accuracy measures reliability of the classification and is calculated by dividing the correctly classified pixels in a category by the all the pixels that were classified in that category. Thus, subtracting user's accuracy from 100 percent gives the commission error or the percentage of misclassified pixels.

Fusing the LIDAR and HyMap data showed overall improved classification accuracy (considering both producer's and user's accuracy) for all categories except stable dune habitat. Stable dune did show improved accuracy for the combined data

classification over HyMap by decreasing omission error by 37% although commission errors showed a slight increase (Fig 2). However, the overall accuracy for stable dune habitat classified from LIDAR was reduced when the combined data were classified. The commission error for stable dune habitat in the combined data set was increased 20% over that for the LIDAR classification alone (Fig 2). Shoreline and beach dune were misclassified as stable dune in the combined classification. Shoreline classification showed improved accuracy with decreased omission and commission errors for the combined classification over LIDAR or HyMap alone. Shoreline was often classified as beach dune in the HyMap classification and as marsh in the LIDAR classification. The most drastically improved classification accuracy was marsh habitat in the combined classification over the LIDAR classification where producer's and user's accuracy improved 76 and 61%, respectively (Table 3). Marsh was frequently misclassified as shoreline in the LIDAR classification. Woodland habitat was classified equally well for all classifications showing a small omission error for the LIDAR classification and a small commission error for the HyMap classification that was reduced to no error for omission or commission when the combined data was classified (Fig 2).

Inclusion of the LIDAR data with the spectral data reduced the misclassification of spectrally similar habitats such as beach dune and shoreline. Also, utilizing spectral data with LIDAR improved separation between classes of similar elevation and maximum height such as shoreline and marsh. Integrating LIDAR elevation data with IKONOS multispectral satellite data (4m GSD) has been shown to improve coastal classifications (water, marsh, tree, sand, road, and buildings) by reducing classification errors as much as 50% for spectrally similar classes such as between road and roof or

marsh and water (Lee & Shan, 2003). Spectral similarities in multispectral Quickbird data (2.5 m GSD) contributed to misclassification of habitats with exposed sand on Fire Island, NY; however, inclusion of GIS vegetation map helped improve classification (Wang, Traber, Milstead, & Stevens, 2003). In addition, HyMap hyperspectral data of Smith Island, VA, acquired at a 4.5 m spatial resolution was used to discriminate 19 classes including a mixture of vegetation types and individual species with 72 to 90% accuracy. (Bachmann et al., 2002). Although spectral overlap and similarities caused misclassification among classes, increasing the number of samples used in classification along with acquiring data later in the growth cycle were cited as possible improvement to the classification on Smith Island (Bachmann et al., 2002).

Historical comparison

In order to improve accuracy and eliminate confusion stable dune habitat was classified using the LIDAR data alone, and masked out of the image prior to running the ML classification with the remaining classes. The 8 HyMap bands derived from the DFA along with the minimum and maximum returns from LIDAR were used to classify the portion of the island covered by both images. The 110 ha area on the north side of the island not covered by the LIDAR data was classified using the 8 HyMap bands alone. Overall accuracy for this classification was 97% with 0.96 K_{hat}.

Table 3. Classification accuracy (producer's) and reliability (user's) for HyMap (H), LIDAR (L), and combined LIDAR and HyMap (C). Overall accuracy and K_{hat} are shown at the bottom of the table.

Habitat	Producer's Accuracy (%)			User's Accuracy (%)		
	H	**L**	**C**	**H**	**L**	**C**
Marsh	77	12	88	100	36	97
Meadow	95	85	89	84	76	91
Stable Dune	63	96	100	77	91	71
Woodland	100	95	100	94	100	100
Beach Dune	77	71	76	46	90	100
Shoreline	35	69	83	63	43	87
	Overall Accuracy (%)			K_{hat}		
Horn Island	74	73	90	0.69	0.67	0.87

Detailed explanation can be found in the results section under classification.
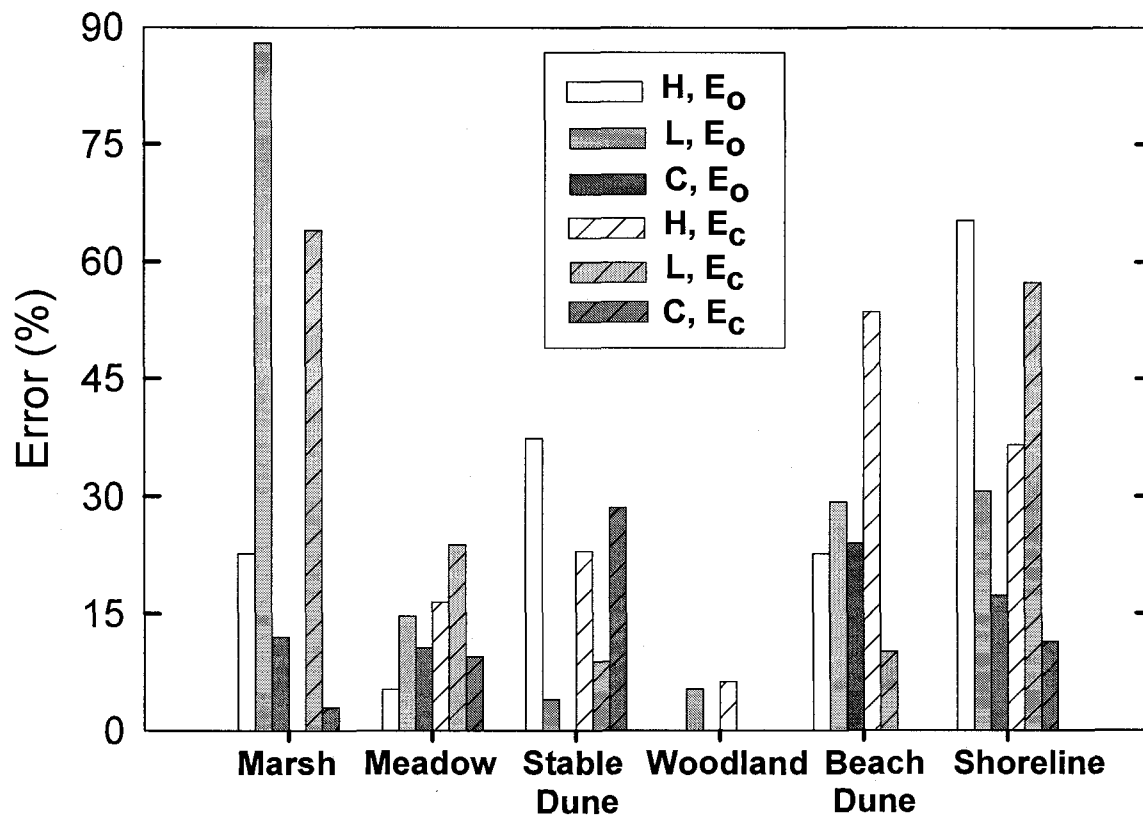
Fig. 2. Classification errors of omission (E_o) and commission (E_c) for each habitat for the

HyMap classification (H), LIDAR classification (L), and the combined LIDAR and

HyMap classification (C).

Although the 1979 classification map was regarded as accurate, the exclusion of microhabitats with no set minimum mapping units allowed for only broad comparisons between classifications. Analysis of the 1979 map indicates that some microhabitats on the order of 200 to 400 m^2 were included in the classification; therefore, exclusion of microhabitats appears to be subjective. The 3 m spatial resolution of the present classification allows for minimum mapping units to be as small as 9 m^2, and increasing the mapping units to 324 m^2 reduced the accuracy of the current classification by 30 percent and reduced K_{hat} by more than half. For consistency in calculations, island and habitat area were calculated from the rasterized vectors for the digitized 1979 vegetation map. The area calculated from the digitized image differed by an average increase of 30 ha per habitat from numbers presented in the 1979 report (Eleuterius, 1979). The difference in calculations is more than likely attributable to differing techniques used to make calculations, and the broad black boundaries delineating the habitats on the 1979 map reducing area measurement for habitats.

Even though the mapping methods varied between the 1979 classification and the current classification, habitat area compared as a proportion of the island area as a whole shows only slight reductions in habitat size for shoreline, beach dune, stable dune, and woodland, and slight increases for marsh and meadow (Table 4). Overall the total vegetation cover on the island expressed as a percentage of the total island area shows only a 2% increase from 1979 to this study. Drastic changes in habitat classification occurred mainly in areas where changes in island geomorphology were the greatest (Fig 3). The eastern end of Horn Island lost approximately 60 ha between 1979 and 2004 resulting in a decline in stable dune and woodland habitat located on the eastern end of

the island (Fig 3). The eastern end of Horn Island experiences erosion with the predominate southeasterly winds and waves responsible for westward direction of the net littoral drift although wave refraction accounts for drift reversal on the re-curving spit of the eastern tip (Otvos & Carter, 2008).

Total island land area between 1979 and 2003 decreased by 154 ha (10.5%), resulting in a -6.4 ha yr^{-1} rate of change. This same rate of change in land area was calculated for Horn Island from aerial photographs between 1976 and 1986 (Byrnes, McBride, Penland, Hiland, & Westphal, 1991). Rates of change and erosion on barrier islands have been attributed to waves, wind, subsidence, extreme episodic events (hurricanes), dredging, sediment diversion, and other human related factors (Craig, Turner & Day, 1979; Douglass, 1984; Otvos & Carter, 2008). Although land area has declined, vegetation as a percent of total land area appears to be more stable. Marsh and meadow habitat did show increased cover between 1979 and 2003; however, this could be attributable to mapping differences. The pond area appears to have declined by 20 ha; although as a percentage of total island area there is no change.

On barrier islands rising sea-level and subsidence are resulting in increased wetlands and vegetation replacement such as low marsh replacing high marsh and high marsh replacing shrubs (Hayden et al., 1995). Also shoreline erosion along with loss of elevation and the fresh water table results in forest die back that can not be replaced unless island rebuilding occurs (Hayden et al., 1995). Eustatic sea-level rise worldwide is between 1 – 2 mm yr^{-1} (Gornitz, 1995); however, subsidence on Horn Island falls somewhere between 5 mm yr^{-1} measured for Waveland, Mississippi located to the west of Horn Island and 1.7 mm yr^{-1} for Dauphin Island (Shinkle & Dokka, 2004) resulting in a

minimum relative sea-level rise of 2.7 mm yr^{-1} to a maximum of 7mm yr^{-1}. Although this comparison shows an increase in meadow and marsh and a decrease in woodland and stable dune differing mapping methods do not provide adequate information to assess the vegetation changes that may have resulted due to relative sea-level rise.

Table 4. Comparison of land area for plant communities, shoreline, and ponds (including lagoons) also expressed as the percent of total island cover for the 1979 vegetation classification map and the combined vegetation classification (97% overall accuracy) produced for this study.

	1979 Area (ha)	1979 %	2003 Area (ha)	2003 %
Pond	105	7	85	7
Shoreline	141	10	113	9
Beach Dune	458	31	345	26
Stable Dune	92	6	31	2
Meadow	288	20	399	30
Marsh	177	12	244	19
Woodland	209	14	96	7
Total Vegetation	1224	83	1115	85
Total Island	1467		1313	

Total vegetation was calculated by adding the land area for beach dune, stable dune, meadow, marsh, and woodland habitats.
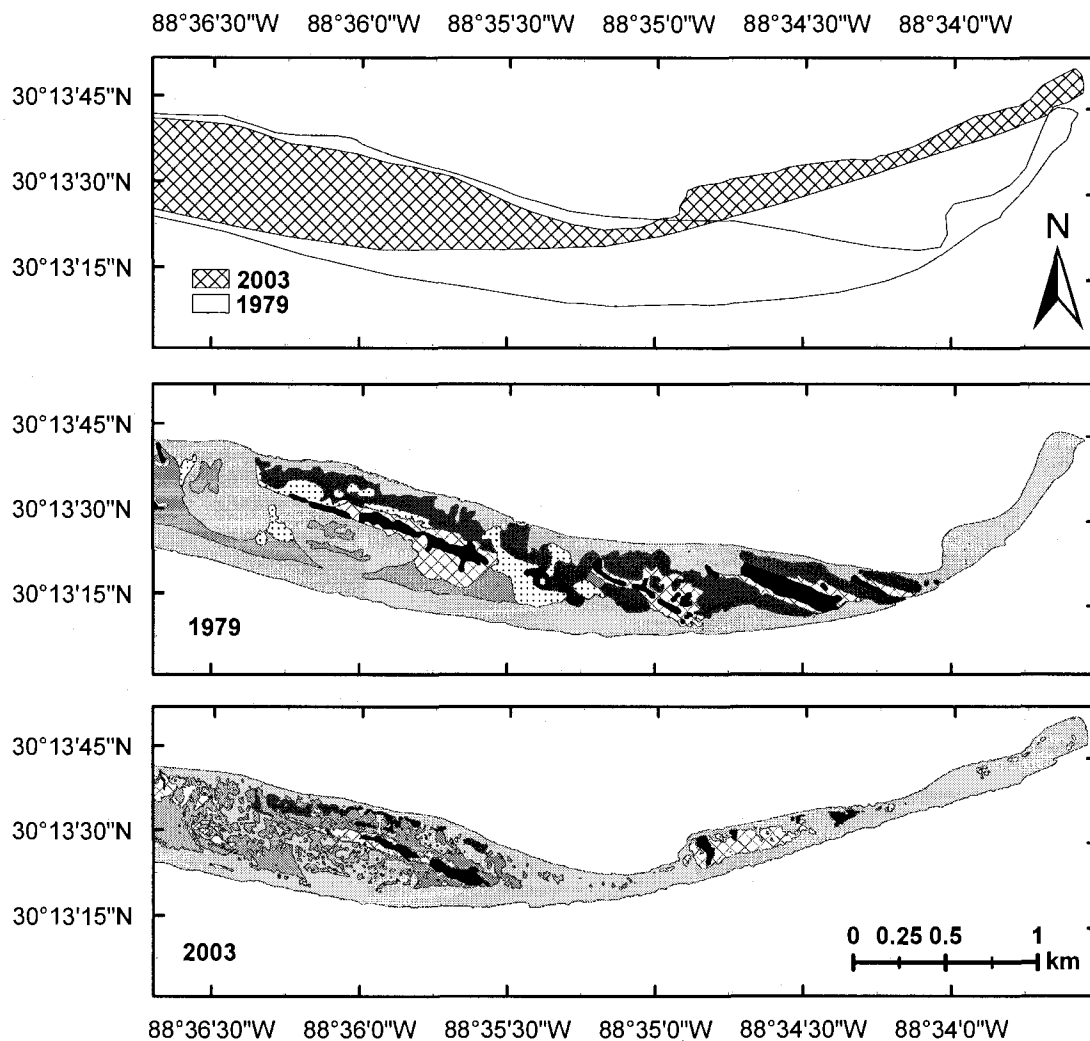
Fig. 3. The top map shows the erosion and re-curving on the eastern end of Horn Island that has occurred since 1979. The middle map is the habitat classification of the eastern end of Horn Island from the 1979 digitized vegetation map, and the bottom map is the current 2003 classification using the combined HyMap and LIDAR data. For both classifications shoreline and beach dunes are shown in light gray, stable dune is dark gray, meadow is medium gray, marsh is cross hatched, woodland is stippled, and ponds are black.

Conclusion

Vegetation composition of habitats appears to be consistent on Horn Island as well as other islands in the Alabama-Mississippi barrier island chain, and also shows similarity with other Northern Gulf of Mexico barrier islands. In comparing the current study with the 1979 vegetation study of Horn Island, marsh and stable dune show the two most prevalent species remaining constant through time. Common species in meadow habitat vary the most between islands, and although the most frequent species in meadow vary from the 1979 study, torpedo grass remains widespread. Fluctuations of distance to fresh water and duration of saturation along with natural disturbance and competition in swale habitat are thought to play key roles in vegetation composition (Rheinhardt & Fraser, 2001). The varying frequency of species in woodland habitat through time reflects the patchiness of the tree-dominated vegetation on Horn Island in that stands range from open woodlands with herbaceous or barren understory to mature dense canopies with thick shrub canopies in the understory. Thus, the frequencies reported by this study as well as other studies may vary based on location of samples and methods used. Although the randomization of samples in this study resulted in only 6 woodland transects, yaupon holly, slash pine, and wax myrtle showed high frequencies in this study and previous studies.

Classification accuracy and reliability in this study was significantly improved by combining spectral and LIDAR data, which has also been found to be the case in other coastal environments (Lee & Shan, 2003). Adding LIDAR to the spectral data helped to separate classes that had similar spectral signals and the spectral data helped separate classes that were similar in elevation or canopy return. Also, combining GIS vegetation

maps with Quickbird data and in-situ spectral data with remotely sensed hyperspectral data has been found to improve classification accuracy on other barrier islands (Bachmann et al., 2002; Wang et al., 2007) Therefore, the classification of land cover on barrier islands may require the combination of multiple layers of heterogeneous data sets for improving accuracy. In addition, the 3 m GSD of the data is essential for delineating and discriminating among habitats that change rapidly over short distances. Classification accuracy and reliability decreased when mapping units were increased to $324\ m^2$ because smaller patches of vegetation were excluded.

Uncertainties from source data, mapping technique, and real world variability led to uncertainties in vegetation change analysis (Janssen, 2004); therefore, with limited knowledge on the uncertainties from the 1979 vegetation map, only broad comparisons were made with the current vegetation map Vegetation and ecosystem changes are linked to variation in changes of elevation in land, sea, and the fresh water table, which are attributable to sea-level rise, storms, and ecological process on barrier islands (Hayden et al., 1995). Relative sea-level rise increases wetlands on barrier islands (Ehrenfeld, 1990) and although marsh and meadow show an increase in coverage, uncertainties in the 1979 map do not allow for assessments based on sea-level rise. However, geomorphological changes, especially on the eastern end of the island, show extensive changes in habitat based on land loss and changing land elevation. Changes in land elevation and morphology as well as position on the barrier island determine exposure to wind, waves, salt spray, storm surges, and distance to fresh water all of which control vegetation composition (Hayden et al., 1995). Overall it appears that

vegetation cover as a percentage of total land area and rate of decrease in land area has remained constant since 1979.

This study indicates the habitat-types on Mississippi Sound barrier islands can be identified and classified based on high-frequency indicator species that are consistent both over time and among islands. Also, improving vegetation classification accuracy on Horn Island at fine spatial scales (3m) can be achieved by including multiple data types that provide heterogeneous information such as LIDAR and spectral data. In addition, despite uncertainties, this study was able to make broad comparisons on vegetation changes that have occurred on Horn Island since 1979 and link some changes in habitat-types to geomorphological changes on the Island. Furthermore, for future studies, classifying vegetation on a general or habitat level and using the same protocols and mapping techniques for all classifications would provide a more accurate way to assess and monitor vegetation on barrier islands.

CHAPTER III

THE USE OF PASSIVE REMOTE SENSING TO ASSESS VASCULAR PLANT

SPECIES RICHNESS ON HORN ISLAND, MISSISSIPPI

Introduction

Biodiversity assessment via remote sensing is becoming a powerful approach in

defining diversity patterns, monitoring change, and aiding conservation efforts (Mooney

& Chapin, 1994; Rey-Benayas & Pope, 1995; Stohlgren et al., 1997). Generally, such

methods rely on the direct detection of organisms or community types or on more indirect

relationships of biodiversity with habitat class along with climate or primary productivity

estimates (Nagendra, 2001; Turner et al., 2003). A useful strategy for assessing

biodiversity has been the deriving of habitat classifications from broad-band satellite data

and relating habitat-type to ground measurements of diversity (Debinski, Kindscher, &

Jakubauskas, 1999; Gould, 2000; Kerr, Southwood, & Cihlar, 2001; Lauver, 1997;

Nagendra & Gadgil, 1999; Oindo, Skidmore, & De Salvo, 2003). To date, most uses of

remote sensing to assess biodiversity have addressed large ground areas at moderate

spatial and spectral resolutions (10-30 m Ground Sample Distance or GSD; bandwidths >

20 nm). Satellite systems including the Landsat TM, ETM+ and Satellite Pour

l'Observation de la Terre (SPOT) High Resolution Visible (HRV) sensors have been used

to estimate species diversity in a variety of habitat-types (Debinski et al., 1999; Gould,

2000; Jorgensen & Nohr, 1996; Kerr et. al., 2001; Lauver, 1997; Oindo et al., 2003; Seto,

Fleishman, Fay, & Betrus, 2004).

With respect to land use and conservation, management decisions are made typically for mesoscale (1-100 km^2) landscapes (Kareiva, 1993; O'Neill et al., 1997; Stoms, 1994). Thus, the development of remote sensing techniques for assessing biodiversity at the mesoscale should prove directly beneficial in natural resource management and biodiversity protection efforts. At mesoscales, a fine spectral resolution may be more important than a greater spatial resolution in characterizing vegetation (Gao, 1999; Thenkabail et al., 2003), revealing features which are useful for directly detecting organisms and discriminating among species (Turner et al., 2003). Recently, airborne HYDICE (HYperspectral Digital Imagery Experiment) data acquired at a 1.6 m GSD with narrow spectral bands (10 nm) was used to spectrally discriminate and classify tropical rainforest tree species (Clark, Roberts, & Clark, 2005; Zhang, Rivard, Sanchez-Azofeifa, & Castro-Esau, 2006). Also, simple ratios of radiance or reflectance in narrow spectral bands of Advanced Visible and Infrared Imaging Spectrometer (AVIRIS) data acquired at a 20 m GSD were found to correlate significantly with species diversity in a 14 km^2 grassland (Carter et al., 2005), and wavelet transformations of EO-1 HYPERION data (30 m GSD) correlated significantly with the Shannon species diversity index for a tropical dry forest (Kalascska et al., 2007).

As highly dynamic landscapes, barrier islands present unique challenges in the development of remote sensing methods for biodiversity assessment. Existing at the land-sea interface, these islands change continually in response to waves, wind, currents, sediment supply, storms, rising sea-level, and coastal subsidence, potentially defining them as important indicators of global climate change (Pilkey, 2003). Along the Atlantic and Gulf of Mexico coasts of the U.S., barrier islands constitute approximately 85% of

the open-ocean shoreline (Stauble, 1989). They protect mainland shores from the higher-energy waves of the open ocean (Snyder & Boss, 2002; Stive & Hammer-Klose, 2004), foster the creation of productive estuaries, coastal wetlands, and aquatic environments (Godfrey, 1976), and supply food and shelter for resident and migratory animals. The barrier island environment favors species that are highly adapted to environmental stressors such as salt spray, saltwater and freshwater flooding, drought, burial by sand, and low soil nutrient content (Lee & Ignaciuk, 1985; Oosting, 1954; Shao et al., 1996). Given present-day expectations that sea-level rise will accelerate (Holgate & Woodworth, 2004; Zhang et al., 2004), tropical storms will increase in frequency and severity (Hayden & Hayden, 2003), and human populations in coastal zones will expand rapidly (USCOP, 2004), efficient methods of monitoring biodiversity on barrier islands will be vital to understanding the impact of global climate change on coastal environments.

Plant species richness, defined as the number of species in a given location, is an essential characteristic of ecosystems (Chapin et al., 2000; Hooper & Vitousek, 1997; Tilman et al., 1997) and its assessment via remote sensing provides a useful measure of biodiversity (Stoms & Estes, 1993). The goal of the present study was to utilize hyperspectral data acquired from an airborne platform at high spatial resolution (HyMap) to assess vascular plant species richness on Horn Island, Mississippi. Primary objectives were to: 1) determine correlations of plant species richness at randomly-selected island locations with relatively simple reflectance indices (band ratios and spectral derivatives); 2) determine correlations of richness with spatial variability in these indices, and 3) evaluate the consistency with which a particular index may correlate strongly with richness among island habitats.

Methods

Study site

Located 18 km seaward of the Mississippi mainland shore, Horn Island (30° 13'N, 88° 40'W) (Fig. 4) was placed under the jurisdiction of the Gulf Islands National Seashore, U.S. National Park Service, in 1971. Designated as a Wilderness Area in the National Wilderness Preservation System, it is one of more than 50 barrier islands that border the northern Gulf of Mexico and contains a variety of habitat-types. These include beach dunes, swales, lagoons, ponds, fresh and saltwater marshes, and maritime forest. All data for this study were acquired prior to Hurricane Katrina (August 29, 2005) when the island was approximately 22 km long (E-W), a maximum of 1 km wide (N-S) and included approximately 1300 ha (1.30 km^2) of land area above mean high-tide level. The climate is humid subtropical with an average air temperature of 12° C in winter and 27° C in summer. Average annual precipitation is 140 cm with a peak in July due mainly to thunderstorms.

Previous Horn Island surveys identified 260 species of vascular plants located in five habitat-types: beach, marsh, meadow, woodland, and stable dune. (Eleuterius,1979). Beach vegetation is dominated by local or pantropical species, with the grasses sea oat (*Uniola paniculata*) and Gulf bluestem (*Schizachyrium maritimum*) comprising 70% of the relative cover (Barbour, Davis, Johnson, & Pavlik, 1987). In marsh habitat, saltmeadow cordgrass (*Spartina patens*) and black needle rush (*Juncus roemerianus*) are most abundant. Meadow or swale habitats, which are found at slightly greater elevation than marshes, are dominated by southern umbrella sedge (*Fuirena scirpoidea*) and torpedo grass (*Panicum repens*) (Eleuterius, 1979). Stable dune habitat is characterized

by high, dry dune ridges occupied by woody goldenrod (*Chrysoma pauciflosculosa*),

beach rosemary (*Ceratiola ericoides*), and rock rose (*Helianthemum arenicola*) (Moore,

Kerlinger, & Simons, 1990). Woodland habitat, which includes the least land area, is

characterized by an overstory of slash pine (*Pinus elliotii*) with occasional sand live oak

(*Quercus geminanta*) and an understory that may be barren to densely covered by the

shrubs wax myrtle (*Myrica cerifera*), yaupon holly (*Ilex vomittoria*), or eastern baccharis

(*Baccharis halimifolia*) (Moore, Kerlinger, & Simons, 1990).
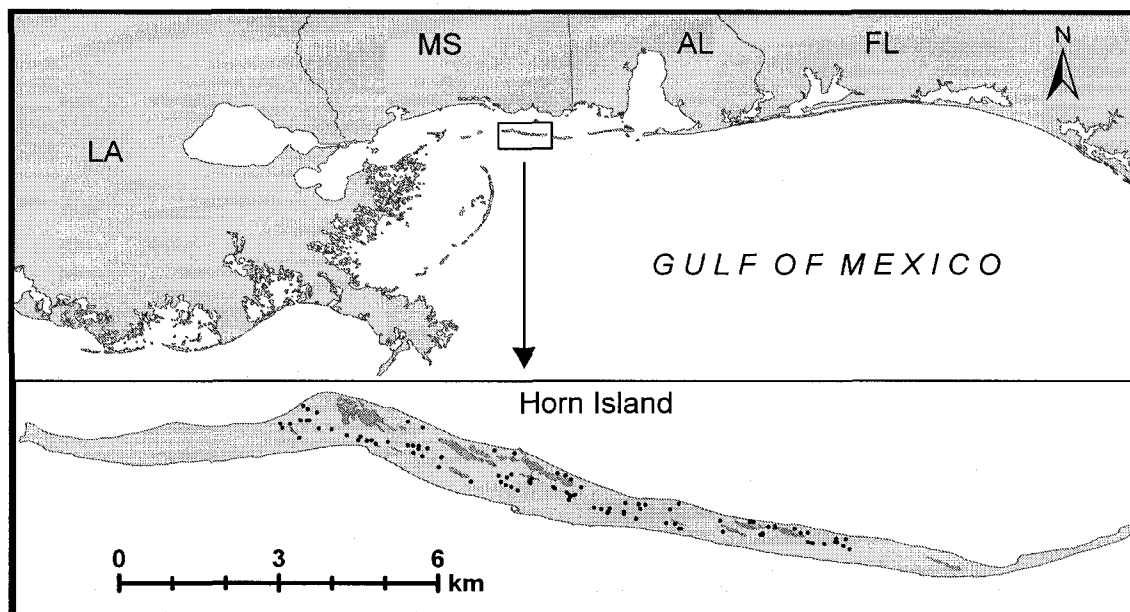
Fig. 4. Map of the northern Gulf of Mexico showing the location of Horn Island,

Mississippi. Zoomed insert of Horn Island indicating randomly-located transects (*n*=95).

The darker gray areas on Horn Island are inland ponds or lagoons. No transects were

located on the eastern and western ends of the island because these areas were subject to

vegetation change between the image acquisition and ground sampling dates

Image data acquisition and pre-processing

Remotely-sensed data combined with ground transect data were used to evaluate relationships of plant species richness with reflectance indices. Hyperspectral imagery of Horn was acquired on October, 15, 2003 by the HyMap airborne imaging system (HyVista Corporation, NSW, Australia). The HyMap sensor employed a rotating scan mirror that constructed an image line-by-line as the aircraft flew forward. Four 32-element detector arrays provided a 126-band data cube that spanned the 450 to 2500 nm spectral range for each pixel in a 512-pixel swath. Full-width-at-half-maximum (FWHM) bandwidths were approximately 15 nm. The above-ground flight altitude of 1400 m produced a 3 m GSD. An on-board GPS provided geographic latitude and longitude information for each pixel (WGS 1984, UTM Zone 16N) stored in an Input Geometry (IGM) file.

HyVista calibrated the data to apparent reflectance using HyCorr, a program similar to the ATmospheric REMoval program (ATREM) (Gao et al., 1992) to account for the effects of atmospheric absorption and scattering. Bands centered at 456, 858, 873, 1390, 1406, 1420, 1952, and 2490 nm were deleted due to strong atmospheric interference, detector overlap or insensitivity, resulting in a 118-channel data cube. To further refine the scaling to reflectance, spectral reflectance for five areas of dry beach sand devoid of vegetation was measured in-situ on Horn using a field-portable spectroradiometer (model ASD-FS, Analytical Spectral Devices, Boulder, CO). Comparison of in-situ reflectance with reflectance output by HyCorr for the same sand areas showed similar spectra differing by approximately 10 percent on average (Fig. 2). Thus, a scaling factor for each spectral band was determined by dividing in-situ

reflectance by image (HyCorr) reflectance representing the same areas. The HyCorr-output data were multiplied by the scaling factor to yield an improved calibration of image data to percentage reflectance. Because geo-location data were available for each pixel, the resulting unrectified data were preserved to avoid spatial resampling of image spectra prior to their use in regressions with species richness.
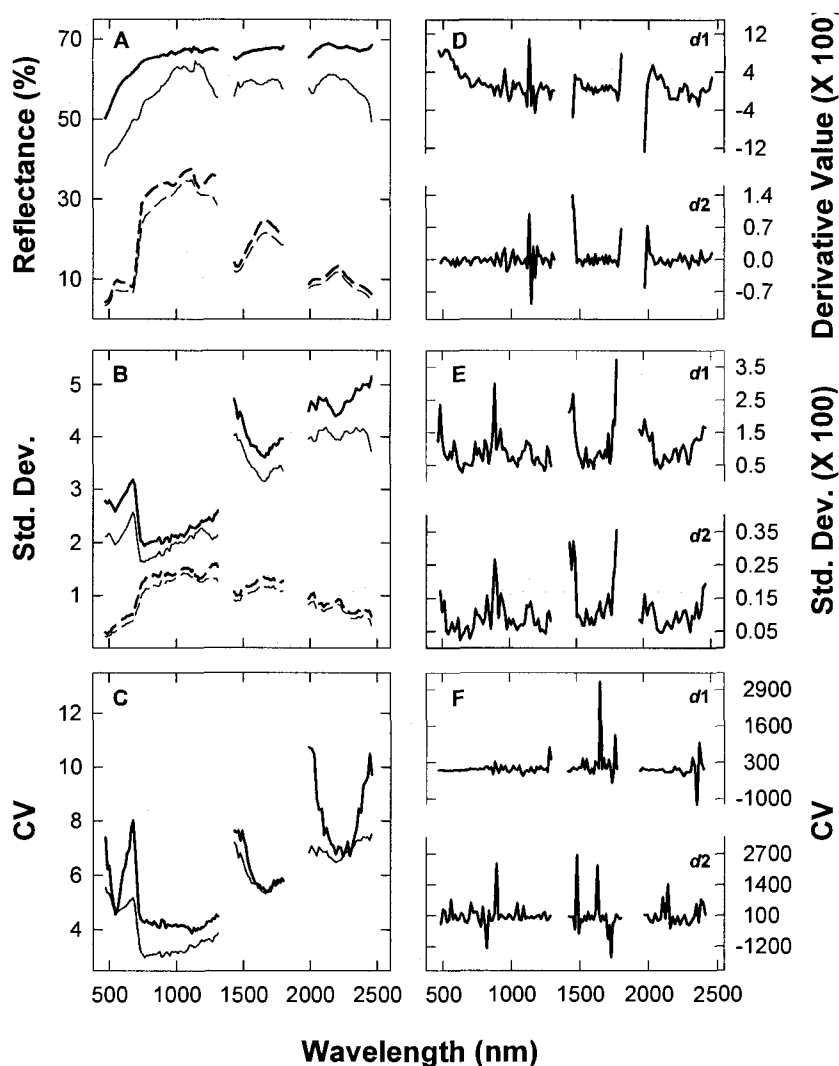
Fig. 5. Pre- and post-calibration reflectance data for dry, white beach sand (n = 10 pixels) and vegetation (n= 10 pixels) along with first and second derivatives for dry, white beach sand (n= 10 pixels). (A) Percent reflectance for original atmospherically corrected HyMap sand (thin solid line) and vegetation (thin dashed line) and calibrated reflectance for sand (thick solid line) and vegetation (thick dashed line). (B) The standard deviation for pre- and post- calibration reflectance data. (C) The coefficient of variation for vegetation (thick solid line) and sand (thin solid line). (D) First and second derivatives for sand and their standard deviation (E) and coefficient of variation (F).

Ground vegetation sampling

Vascular plant species richness was sampled for 95, 15 m line transects that were established at random locations (Fig. 4). One flight line contained 95 of the original 100 transects and therefore the 95 transects were measured in this study. Using transects from one flight line eliminated affects of variations in illumination that are visual between flight lines. Approximately one year elapsed between HyMap image acquisition and the onset of ground vegetation sampling. During this time, a fire on the western end of the island (2003) and storm overwash of the extreme eastern end in Hurricane Ivan (2004) potentially altered species composition. Thus, the western and eastern ends of the island were not sampled (Fig. 4). Also, beach dunes were eliminated from study because they were the only habitat-type in which significant changes in vegetative cover might have occurred during a storm-free year. Otherwise, there was no indication of change in species composition on the remainder of the island. Horn Island vegetation is dominated by evergreen species. Other than senescence in annual plants, the vegetation was vigorous and not exposed to drought between image acquisition and the completion of ground sampling. Transect sampling began in November, 2004 and continued through May, 2005. Spot-checks in April and May, 2005, of transects sampled during the autumn and winter months verified that species composition had remained consistent through the end of the sampling period. Random points on the island derived from the georectified HyMap image (ENVI v. 4.2) were imported to a Trimble GPS receiver (model GeoXT, Trimble Software, Sunnyvale, CA) for use in establishing field transect locations (Fig. 4). Once a point was located in the field it became the center of a 15-m line transect. Habitat-type at transect center was defined according to the Horn Island vegetation classification

system (Eleuterius, 1979). Transect azimuth was directed toward the nearest habitat transition (e.g., woodland to meadow) to capture species richness in transition zones as well as in the more clearly-defined habitat-types. In transition zones, species that are characteristic of a given habitat-type are found mixed with those of an adjacent, different habitat-type. The randomization of transect location resulted in the following number of transects per habitat-type: marsh (10), meadow (18), stable dune (37), woodland (6), and transition zone (24). Sampling was limited to the imaginary vertical plane which contained the transect line. Only species which intersected the plane were counted. A species was counted only once regardless of its abundance along the transect. Additional data recorded for each transect included percent bare soil (percentage of total transect length which intersected sky-exposed bare soil), GPS locations of transect end points and photographs taken from each end point. Percent vegetative ground cover was determined as 100 minus percent bare soil. Transected areas were covered predominantly by either live vegetation or bare soil. On ground not covered by live vegetation, leaf litter and other detritus was distributed sparsely atop white sand and thus was unlikely to have influenced remotely-sensed spectra significantly at the 3-m GSD. Thus, the small percentage of ground covered by detritus exposed to the sky was not determined.

Data analysis

Ground transect geolocations layered over the imagery were used in extracting reflectance spectra from 5 – 11 HyMap pixels (3 m GSD) per transect. For each transect, mean and coefficient of variation (CV) were computed for reflectance per band (R), all-possible two-band ratios of R, first and second R derivative per band interval ($d1$, $d2$), and all-possible two-band ratios of $d1$ and $d2$ (Excel 2003, Microsoft Corporation.,

Redmond, WA). First derivatives (d1) were approximated by dividing the difference in data value between spectrally adjacent bands by the corresponding difference in band central wavelength (Tsai & Philpot, 1998). Second derivatives (d2) were determined likewise from d1 spectra. Spectral data were not smoothed or filtered prior to derivative analysis because the 15 nm bandwidth and averaging the 5-11 derivative spectra per transect reduced data noise substantially (Fig. 5). Also, the finite-difference approach eliminated the possibility of introducing errors which can result from curve-fitting or filtering procedures (Tsai & Philpot, 1998).

The relationship of species richness with mean R or a given derived variable was determined separately for each habitat-type by simple linear regression, the resulting adjusted r^2 and standard error of the estimate (s). An index that yielded a high r^2 and low s in regression with richness was not selected as potentially useful unless at least two spectrally adjacent indices yielded approximately equal r^2. This procedure greatly reduced the probability that a selected index regressed strongly with richness merely by chance.

Results

Species richness and habitats

Although 260 vascular plant species were reported previously for Horn Island (Eleuterius, 1979), only 69 species were found in the present study (Table 5). However, beach dunes were not sampled and our line-transect approach differed from earlier sampling methods. These factors may account for some portion of the apparent decline in Horn Island species richness over the past several decades.

Number of species per transect ranged from 0 to 12. At the lowest elevations, marsh habitat exhibited flooded to near-saturated soils with nearly 100 percent cover by vegetation. Richness averaged four species per transect (Table 5) dominated by black needle rush and saltmeadow cordgrass. Woodlands were dominated by slash pine with high vegetative cover and averaged 5 species per transect. In contrast, stable dunes included the greatest percentage of bare soil (sand) and were dominated by low shrub vegetation with a low richness of 4 species per transect. Meadows and transition zones averaged 7 species per transect (Table 5). Meadows were characterized primarily by herbaceous vegetation dominated by torpedo grass and soils that varied from a wet peat covered by vegetation to exposed sand. Transition zones, located primarily between meadows and stable dunes and secondarily between marsh and stable dunes, averaged 7 species per transect. Transition-zone soils were often moist and vegetation cover was approximately 70 percent. This coverage was greater than in meadows and stable dunes but less than in woodlands and marshes.

Table 5. Total number of species recorded for habitat-type and all habitats combined along with mean number of species and percent cover with standard deviation shown in parentheses. The randomization of 95 transects resulted in the following number of transects per habitat-type: meadow (18), relict dune (37), marsh (10), woodland (6), and transition zone (24).

Habitat-type	Total Species	Mean Species per Transect	Cover (%)
Marsh	16	4.4 (1.8)	98 (6)
Meadow	35	6.8 (0.8)	63 (30)
Stable Dune	32	4.0 (1.4)	58 (27)
Transition Zone	39	7.1 (2.1)	72 (23)
Woodland	12	5.0 (2.2)	88 (15)
Habitats combined	69	5.6 (2.4)	69 (27)

*Previously, 260 vascular plant species were recorded on Horn Island (Eleuterius 1979).

**95 transects from one flight line were used from this study avoid illumination gradients that occur in the imagery between flight lines.

Regression results and index fidelity

Regression analysis indicated significant ($p \leq 0.05$, maximal adjusted r^2) relationships of plant species richness with each of 23 indices that were based on within-transect mean and 22 indices based on within-transect CV. As a group, these indices (45 in total) incorporated 10 visible-spectrum (ca. 400 nm – ca. 700 nm), 23 near-infrared (ca. 700 nm – ca. 1300 nm), and 26 mid-infrared (ca. 1300 nm – ca. 2500 nm) HyMap bands. Ranges in adjusted r^2 for these relationships were 0.28 – 0.98 and 0.31 – 0.98 for mean-based and CV-based indices, respectively. However, regression analysis alone provided no indication of potential biophysical linkages between richness and index

value for a given habitat-type, other than the generally-known sensitivities of the visible,

near-infrared and mid-infrared spectra to leaf pigmentation, leaf area or biomass, and

water, respectively (Carter, 1991; Penuelas, Pinol, Ogaya, & Filella,1997; Thenkabail,

Enclona, Ashton, & van der Meer, 2004). Thus, a test of index fidelity, based on the

consistency of index response to changes in plant and environmental moisture, was

applied to each of the 45 indices. The test required that the value of a given index must

respond in a consistent manner, i.e., consistently increase, decrease or remain essentially

unchanged, as moisture level increased in each of the following three cases: 1) increasing

relative water content (RWC) in a leaf of *Magnolia grandiflora* (data from Carter, 1991);

2) increasing ray pathlength through thin layers of pure liquid water (modeled after

Downing, Carter, Holladay, & Cibula, 1993, using absorption coefficients from Hale and

Querry, 1973), and 3) increasing relative soil moisture content in the progression from

surf zone to dry beach sand on Horn Island (from the HyMap spectra). Spectral

reflectance data used in cases (1) and (2) were re-sampled to HyMap central wavelengths

and FWHM bandwidths (ENVI v4.2). Only high-fidelity indices, those for which index

value responded in a consistent manner in all three cases, were selected as being

potentially robust indicators of plant species richness within a given habitat-type (e.g.,

Fig. 6). This conservative approach insured that 1) the signal strength of a selected index

relative to random noise was sufficiently high to yield a consistent response to a highly-

variable yet well-documented biophysical influence on landscape reflectance, and 2) the

comparative sensitivity or insensitivity of a selected index to environmental and plant

moisture would be known, thus facilitating a biophysical interpretation of regression

results.

Fidelity testing eliminated all but 7 of the initial 45 indices selected from regression analysis alone, including all indices for which the r^2 in relationship with richness was less than 0.38 or greater than 0.90. The 7 high-fidelity indices included 2 based on within-transect mean and 5 based on within-transect CV. As a group, these incorporated 2 visible, 7 near-infrared and 4 mid-infrared HyMap bands. Richness in marsh and woodland habitats was related to band ratios of mean transect R which incorporated mid-infrared wavelengths greater than 2100 nm (Table 6). R_{618}/R_{2475} for marsh was highly sensitive to moisture whereas R_{2103}/R_{2279} for woodland was comparatively moisture-insensitive (Table 6). Derivative-based index means yielded no high-fidelity correlations with richness.

Within-transect spatial variability (CV) in index value correlated not only with richness in marsh and woodlands but also in meadows and transition zones (Table 6). As with results for transect means (Table 6) marsh was the only habitat-type in which richness correlated with the CV of a moisture-sensitive index (R_{514}/R_{2459}) (Table 6, Fig. 7). In contrast, richness in meadows, transition zones and woodlands correlated with the CV of moisture-insensitive indices. The relationship of richness with the CV of R_{904} in woodland habitat was the only case overall in which reflectance per se correlated with richness. Derivative-based index CVs yielded no high-fidelity correlations with richness.
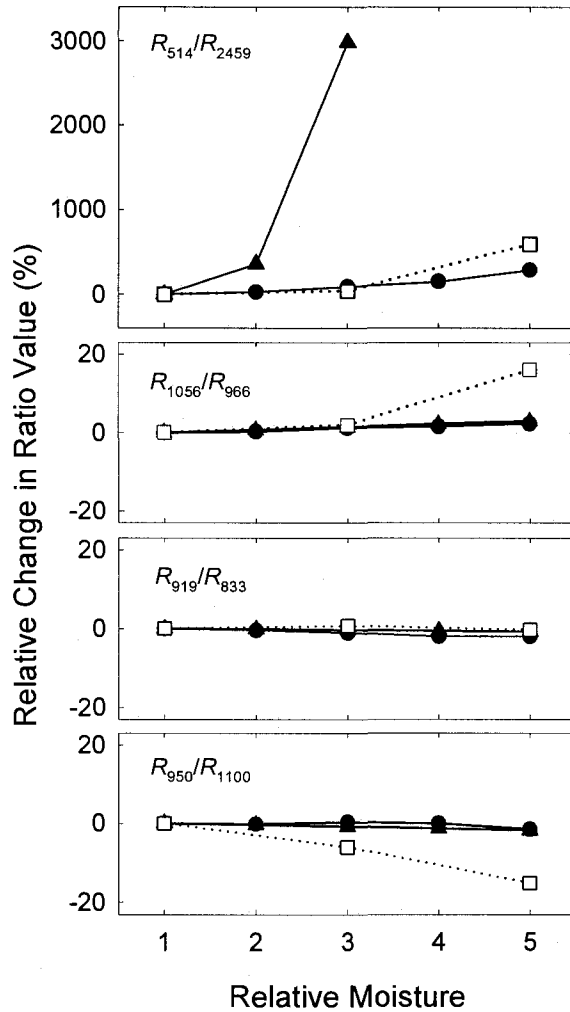
Fig. 6. High index fidelity demonstrated by consistent responses to changes in plant and environmental moisture. Relative change in ratio value is shown as a percentage of driest-state value (Relative Moisture = 1) for : a leaf of *Magnolia grandiflora* at 5, 25, 50, 75 and 100% relative water content (circles) (after Carter, 1991); absorption pathlengths of 0.005, 0.25, 0.50, 0.75 and 1.0 mm through pure liquid water (triangles) (after Downing et. al., 1993) and white beach sand sampled from the HyMap data at 10 m (dry), 3 m (intermediate) and 0 m from the surf zone (wet) (squares). Note the different graph scaling for R_{514}/R_{2459}, by far the most sensitive of these ratios to plant or environmental moisture. In contrast, R_{919}/R_{833} was virtually insensitive to moisture.

Table 6. Adjusted coefficient of determination (r^2), standard error of the estimate (s, species per transect) and probability of a greater F statistic (Pr>F) from simple linear regressions of plant species richness per transect with transect mean and within transect spatial variability (CV) in R and R band ratios for Horn Island habitats. Sensitivity of the index to environmental and plant moisture is given as the relative change in index value (%, absolute value) as the absorption pathlength through pure liquid water is increased from 0.05 mm to 0.25 mm.

Habitat	Variable	Adjusted r^2	s	Pr > F	Rel. Sensitivity (%)
Mean, R Band Ratio					
Marsh	R_{618}/R_{2475}	0.74	0.7	0.001	429
Woodland	R_{2103}/R_{2279}	0.90	0.7	0.003	13
CV, R					
Woodland	R_{904}	0.68	1.2	0.02	0.1
CV, R Band Ratio					
Marsh	R_{514}/R_{2459}	0.69	0.8	0.002	359
Meadow	R_{1056}/R_{966}	0.39	2.2	0.004	0.6
Transition	R_{919}/R_{833}	0.38	1.6	0.001	0.2
Woodland	R_{950}/R_{1100}	0.90	0.7	0.002	0.4

Results shown represent maximal r^2 for each habitat. Band central wavelength (nm) is shown in subscript.
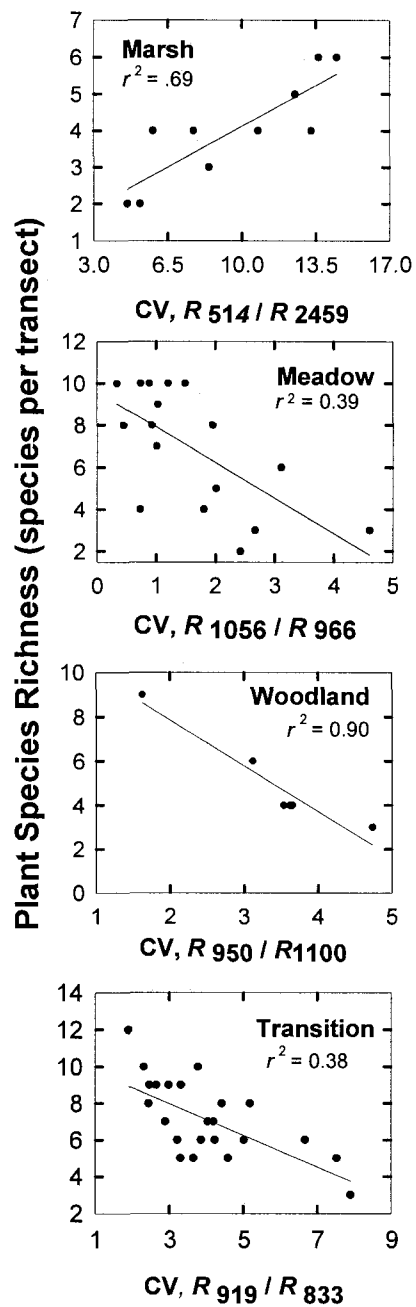
Fig. 7. Regression of plant species richness per transect with the index which produced

the greatest r^2 for a given habitat. The probability of a greater F was $p \leq 0.004$ for all

regressions shown

Discussion and conclusions

Plant species richness, the number of species found in a given location was related to both mean- and spatial variability indices in marsh and woodland habitats; however, richness in meadow and transition zone habitats was significant only for spatial variability in R. No single index provided a best-fit estimation of richness within individual habitat-types. When data for all habitat-types were combined, plant species richness did not correlate significantly with remote sensing indices based on within-transect spatial means or variability. The dependence on habitat-type for the estimation of richness is likely due to the fact that habitat types have similar structural attributes (e.g. leaf, canopy and background features) that contribute to the reflectance signal. And although some studies have found derivatives to be useful in identifying individual species (Gong, Pu, & Yu, 1997; van Aardt, & Wynne 2001), this study found that derivatives or derivative ratios that correlated with species richness did not responded consistently to changes in water content. The lack of derivatives to improve identification of individual species has also been reported for trees in a tropical rainforest (Zhang et al., 2006).

Hyperspectral data has been found to be advantageous over broad-band multispectral data in estimating and classifying vegetation characteristics (Thenkabail et. al., 2004) and identifying individual tree species (Clark et. al., 2005). The results of this study indicate that a fine spectral resolution is also important for estimating plant species richness in specified habitat-types. This is especially true for within transect spatial variability indices for meadow, woodland, and transition zone were two-band ratios in the near infrared were found to be significant at estimating plant species richness.

Multispectral data such as Landsat, Quickbird, and IKONOS contain only one broad-band spanning the near infrared. Also, the middle infrared was significant at estimating plant species richness for marsh and woodland, and often commercial broad-band satellite data such as Quickbird and IKONOS do not cover the mid-infrared region.

Both the CV and mean band ratio indices for marsh were sensitive to changes in water content. On Horn Island, marsh located in areas frequently inundated by water consist mainly of black needle rush. However, in marsh edges along tidal lagoons smooth cordgrass (*Spartina alterniflora*) may sometimes make up 0.15 m of the fringing emergent vegetation in marsh, and occasionally cat tail (*Typha angustifolia*) may be present on the edge of ponds both transitioning to black needle rush beyond the fringing vegetation. Salt marsh plants are affected by the soil oxygen level, water inundation, nutrient availability, accumulation of toxins, and salinity of the soil and water (Garcia, Marañón, Moreno & Clemente, 1993). At increasing distance and elevation from the water the numbers of species in marsh habitat increases as abiotic factors become favorable for more species. The relationship of species richness in marsh with mean R_{618}/R_{2475} show that number of species decrease with increasing moisture or water content, and the relationship with CV of R_{514} / R_{2459} indicates that spatial variability of environmental moisture plays role at predicting species richness in marsh.

Woodland transects exhibiting a greater number of species showed a more developed canopy. Multi-layered organization enhances structural complexity in forest canopies and increased vertical complexity is generally associated with high plant species diversity in forests (Bazzaz, 1975; Ishii, Tanabe, & Hiura, 2004). The transect with the greatest richness had both a slash pine overstory and a dense yaupon holly and wax

myrtle sub-canopy along with partial ground coverage by saltmeadow cordgrass about 1 m in height. The other transects were characterized by only a partial sub-canopy of shrubs and more bare soil exposure. Meadow habitat consists of both low herbaceous vegetation along with some shrubs and occasional broadly-spaced slash pine. Meadow transects with the greatest number of species are comprised of both herbaceous vegetation and shrubs with mostly complete cover by vegetation. Although transition zones occur between adjacent habitats, transects with more transect line occurring in the meadow or high marsh showed greater species richness. The transition zone exhibiting the largest number of species was located between high marsh and meadow and showed almost no bare soil exposure. Species richness in woodland was significantly related to mean reflectance that was not responsive to changes in water content, and species richness in woodland, meadow, and transition zone were significantly related to CV ratios in the near-infrared that were also not responsive to changes in water content. The near-infrared is known to be sensitive to biomass and LAI (Jensen, 2005). The response of these habitats to CV band ratios in the near-infrared show the number of species increases as variability in vegetation composition increases and vegetation cover increases. The woodland mean reflectance ratio also indicates that as vegetation cover increases species richness increases.

Thus, among the 7 indices that were found useful in richness estimation (Table 5), both the CV and mean band ratio indices for marsh were sensitive to changes in water content and the other 5 indices for woodland, meadow, and transition zone were not responsive to changes in water content. These indices indicate that environmental moisture along with moisture in leaves and soil are important for estimating species

richness in marsh, and LAI and biomass are important for estimating the number of species in woodland, meadow, and transition zone. Whereas these results focus on assessing species richness, measured by the number of species in a given location, others have used hyperspectral data to identify individual tree species (Clark et al., 2005; Zhang et al., 2006). Clark et al. (2005) found spectral bands bordering near-infrared moisture absorption features along with wavelengths in the middle-infrared particularly useful in identifying individual tropical rainforest tree species at pixel and crown scales. The middle-infrared was significant in estimating plant species richness using narrowband AVIRIS data for a tallgrass prairie (Carter et. al., 2005) and HYPERION data for a dry neotropical rainforest (Kalacska et al., 2007).

Clearly, a fine spectral resolution and use of near-to-mid infrared spectral bands were important in assessing plant species richness for Horn Island habitats. Overall, simple indices based on terrain spectral features significantly estimated plant species richness in marsh and woodland habitat. However, the advantage of quantifying within-transect spatial variability in index value was demonstrated in the capability of R ratios to estimate richness for four of the five habitat-types. These results are promising to the remote estimation of species richness from hyperspectral data.

CHAPTER IV

ESTIMATING VASCULAR PLANT SPECIES RICHNESS ON HORN

ISLAND, MISSISSIPPI USING SMALL FOOTPRINT AIRBORNE LIDAR

Introduction

Biodiversity assessment through the use of remote sensing is becoming a

powerful approach in defining diversity patterns, monitoring change, and aiding in

conservation efforts (Mooney & Chapin, 1994; Rey-Benayas & Pope, 1995; Stohlgren et

al., 1997). Generally, such methods rely on the direct detection of organisms or

community types or on indirect relationships of biodiversity with habitat class along with

climate or primary productivity estimates (Nagendra, 2001; Turner et al., 2003). A useful

strategy for assessing biodiversity has been deriving habitat classifications from broad-

band satellite data and relating habitat-type to ground measurements of diversity

(Debinski et al., 1999; Gould, 2000; Kerr et al., 2001; Lauver, 1997;Nagendra & Gadgil,

1999; Oindo et al., 2003). However, narrow-band hyperspectral data has recently been

used to spectrally discriminate and classify tropical rainforest tree species (Clark et al.,

2005; Zhang et al., 2006) and estimate species richness in grassland (Carter et al., 2005)

and tropical dry forest habitat (Kalascska et al., 2007).

Although remotely sensed data acquired by passive optical systems are

increasingly a critical component in biodiversity assessments, LIDAR (light detection

and ranging) may provide improved assessments owing to its greater fidelity in

quantifying topographic features and three-dimensional vegetation structure (Lefsky et

al., 2002). LIDAR operates by recording the time elapsed between the emission of a

laser pulse toward the target and detection of the backscattered pulse (return time).

Topographic elevation and height differences among ground objects are computed given

return time, the speed of light and flight altitude (Dubayah & Drake, 2000). For

terrestrial applications, LIDAR lasers operate typically in the 900 – 1064 nm wavelength

range so that a detectible backscattered pulse (high signal-to-noise) may be received from

the ground or vegetation (Lefsky et al., 2002, Raber, Jensen, Schill, & Schuckman,

2002). LIDAR data have been used to accurately estimate vegetation height, cover,

canopy structure, leaf area index, and above-ground biomass in forest applications

(Dubayah & Drake, 2000; Lefsky et al., 1999;Nelson, Oderwald, & Gregoire, 1997). In

addition, vegetation height has been determined successfully in wetland (Genc, Dewitt, &

Smith, 2004; Genc, Smith, & Dewitt , 2005), shrub (Streutker & Glenn, 2006), and

coastal woodland habitats (Nayegandhi, Brock., Wright, & O'Connell, 2006). The

vertical distribution of returns has also provided a means to classify vegetation habitats

using LIDAR alone (Raber *et al*. 2002) or in conjunction with spectral data (Hill &

Thomson, 2005; Lee & Shan, 2003).

The structural arrangement of vegetation influences the distribution and

interactions of animal species. Relationships of faunal species diversity with structural

characteristics are dependent on the scales specific to the habitat requirements (eg. food,

cover from predators, or reproduction) of the species of interest (Tews, et al. 2004).

Canopy architecture and heterogeneity influence avian (MacArthur & MacArthur, 1961;

Riffel, Keas, & Burton, 2001), mammal (Williams, Marsh, & Winter, 2002), and insect

(Knops et al., 1999) species diversity. In addition, experiments show architectural

complexity and canopy layering is greater for species-diverse assemblages (Naeem,

Thompson, Lawler, Lawton, & Woodfin, 1995), and species-diverse canopies in marsh are not only taller but show increased layering as well (Keer & Zedler, 2002). The use of LIDAR to characterize habitat heterogeneity at spatial scales that are often difficult and time consuming to measure in the field may provide an efficient method for predicting both plant and animal species diversity. Indeed, the vertical distribution of canopy elements determined by LIDAR was shown to be a strong predictor of avian species diversity (Goetz, Steinberg, Dubayah, & Blair, 2007).

As highly dynamic landscapes, barrier islands present unique challenges in the development of remote sensing methods for biodiversity assessment. Existing at the land-sea interface, these islands change continually in response to waves, wind, currents, sediment supply, storms, rising sea-level, and coastal subsidence, potentially defining them as important indicators of global climate change (Pilkey, 2003). Along the Atlantic and Gulf coasts of the U.S., barrier islands constitute approximately 85% of the open-ocean shoreline (Stauble, 1989). They protect mainland coasts from the high energy waves of the open ocean (Snyder & Boss, 2002; Stive & Hammer-Klose, 2004), foster the creation of biologically productive estuaries, coastal wetlands, and aquatic environments (Godfrey, 1976) and supply food and shelter for resident and migratory animals. The barrier island environment favors species that are highly adapted to environmental stressors such as salt spray, saltwater and freshwater flooding, drought, burial by sand, and low soil nutrient content (Lee & Ignaciuk, 1985; Oosting, 1954; Shao et al., 1996). Expectations are that sea-level rise will accelerate (Holgate & Woodworth, 2004; Zhang et al., 2004), tropical storms will increase in frequency and severity (Hayden & Hayden, 2003) and human populations in coastal zones will expand rapidly (USCOP,

2004). These current and anticipated pressures define a pressing need for efficient methods of monitoring biodiversity on barrier islands.

Plant species richness, defined as the number of species in a given location, is an essential characteristic of ecosystems (Chapin et al., 2000; Hooper & Vitousek, 1997; Tilman et al., 1997) and its assessment via remote sensing provides a useful measure of biodiversity (Stoms & Estes, 1993). The goal of this study was to utilize the vertical distribution of airborne multiple-return LIDAR to directly evaluate vascular plant species richness on Horn Island. Primary objectives were to 1) determine correlations of plant species richness at randomly-selected island locations with vertical distribution descriptors such as mean, standard deviation, and range, and 2) determine correlations of plant species richness with vegetation height expressed at each 10th percentile above the minimum as well as ratios of percentiles.

Methods

Study site

Horn Island, Mississippi (30° 13'N, 88° 40'W) (Fig. 8) was placed under the jurisdiction of the Gulf Islands National Seashore, US National Park Service, in 1971. Designated as a Wilderness Area in the National Wilderness Preservation System, it is one of more than 50 barrier islands that border the northern Gulf of Mexico and contains a variety of habitats including beach dunes, swales, lagoons, ponds, fresh and saltwater marshes, and maritime forest. The island is located 18 km seaward of the Mississippi mainland shore. Prior to Hurricane Katrina (August 29, 2005), when data were acquired for this study, the island was approximately 22 km long (E-W), a maximum of 1 km wide (N-S) and included approximately 1300 ha of land area above mean high-tide level. The

climate is humid subtropical with an average air temperature of 12° C in winter and 27° C

in summer. Average annual precipitation is 140 cm with a peak in July due mainly to

thunderstorms.
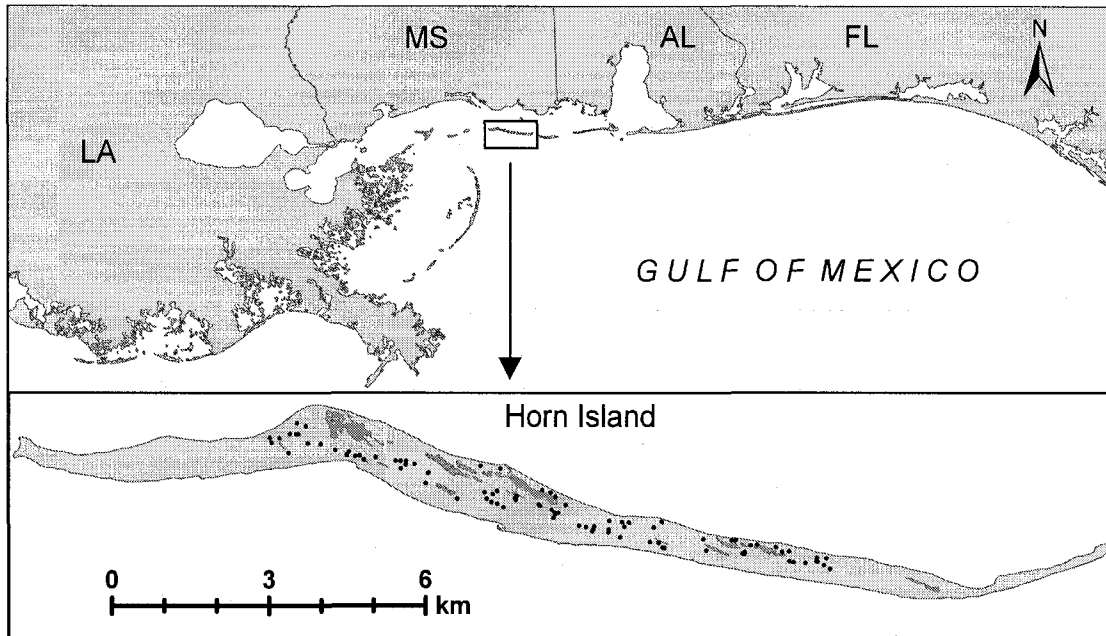
Fig. 8. Map of the northern Gulf of Mexico and Horn Island, Mississippi. The expanded

map of Horn indicates the random placement of 90, 15-m line transects established for

ground-sampling of plant species richness. The LIDAR data did not cover a 110 ha

section on the north side of the island and therefore, only 90 of the original 100 transects

were used in this study. Darker-gray areas represent inland ponds or lagoons. No

transects were established on the eastern and western ends of the island because these

areas were subject to vegetation change during the interval between image acquisition

and ground sampling

Previous surveys identified 260 species of vascular plants located in 5 habitats: beach, marsh, meadow, woodland, and stable dune, on Horn Island (Eleuterius, 1979). The beach vegetation is dominated by local or pantropical species and the grasses sea oat (*Uniola paniculata*) and Gulf bluestem (*Schizachyrium maritimum*) comprise 70% of the relative over (Barbour et al., 1987). Saltmeadow cordgrass (*Spartina patens*) and black needle rush (*Juncus roemerianus*) are the most abundant marsh species. Meadow or swale habitats, which are found at slightly greater elevation than marshes, are dominated by southern umbrella sedge (*Fuirena scirpoidea*) and torpedo grass (*Panicum repens*) (Eleuterius, 1979). Stable dune habitat is characterized by high and dry dune ridges occupied by woody golden rod (*Chrysoma pauciflosculosa*), beach rosemary (*Ceratiola ericoides*) and rock rose (*Helianthemum arenicola*) (Moore et al., 1990). Woodland habitat, which includes the least land area, is characterized by an overstory of slash pine (*Pinus elliotii*) with occasional sand live oak (*Quercus geminanta*) and an understory of barren areas to dense tickets of wax myrtle (*Myrica cerifera*), yaupon holly (*Ilex vomittoria*) and eastern baccharis (*Baccharis halimifolia*) (Moore et al., 1990).

Image data acquisition and pre-processing

LIDAR data in ASCII format containing x, y, and z coordinates for each laser pulse return was provided by the NOAA Coastal Services Center, Charleston, SC. It was acquired over Horn Island in April, 2004, by the Joint Airborne LIDAR Bathymetry Technical Center of Expertise, U.S. Army Corps of Engineers, using the Compact Hydrographic Airborne Rapid Total Survey (CHARTS) system. Laser pulses were emitted at 10 kHz with a wavelength of 1064 nm. The aircraft flew at 400 m above ground level resulting in a spot density per flight line of less than 1 m. Only the first and

last returns per pulse were recorded. Multiple passes over each flight line increased the coverage of returns. An onboard GPS system provided the geographic latitude and longitude (x and y coordinates, NAD 1983, UTM Zone 16N,) of each spot. Vertical return data were recorded in NADV 1988 (z coordinate). Based on information supplied with the LIDAR data and instrument specifications a horizontal accuracy of 0.8 m and vertical accuracy 0.15 m was expected. Previous field tests showed these reported accuracies to be conservative (LaRocque, Banic, & Cunningham, 2004).

Ground vegetation sampling

Vascular plant species richness was sampled for 90, 15-m line transects that were established at random locations (Fig. 8). A 110 ha section on the north side of the island was not covered by the LIDAR data; therefore, only 90 transects of the original 100 transects were used in this study. Approximately 6 months elapsed between LIDAR data acquisition and the onset of ground vegetation sampling. However, Horn Island vegetation is dominated by evergreen species and other than some annual plant senescence, the vegetation was healthy and not apparently exposed to stress from drought between the time of image acquisition and ground sampling. The western and eastern ends of the island were not sampled (Fig. 8) because a fire in 2003 and storm overwash from Hurricane Ivan in 2004 potentially altered vegetation composition. Also, beach dunes were eliminated from study as the only habitat-type on the island in which a significant change in vegetation composition might occur during a storm-free year. Sampling of transects began in November 2004 and continued through May 2005 as sampling frequency was highly dependent on winds, weather and tides. Transects sampled in the winter months were spot-checked in April and May, 2005 to ensure

consistency in vegetation composition during the sampling period. Random points

derived from a georectified island image (ENVI v. 4.2) were imported to a Trimble GPS

receiver (model GeoXT, Trimble Software, Sunnyvale, CA) to establish the transect

locations. Once a point was located in the field it became the center of a 15-m line

transect. The habitat classification of the center point was noted according to the Horn

Island vegetation classification system (Eleuterius, 1979) and transect azimuth was

oriented toward the nearest habitat transition. This method was designed to capture

species richness in transition zones, areas of mixed habitat-type species located between

adjacent habitats, as well as pure habitat types. Randomization of transect location

resulted in the following number of transects per habitat-type: meadow (16), stable dune

(37), marsh (10), woodland (5), and transition zone (22). Ground data recorded for each

transect included percent bare soil, species presence, habitat-type, and geographical

location. Regardless of its abundance, a species was counted only once per transect.

Data analysis

The ASCII file containing the x, y, and z coordinate of each return was converted

to a shapefile (ArcMap v. 9.1, ESRI Corporation, Redlands, CA). The extents of each

transect including a surrounding 3-m buffer was layered over the data and returns that fell

within the designated buffer were exported. For each transect the return minimum,

maximum, range, mean, and standard deviation was calculated. Height percentiles in

increments of 10 above the minimum (zero) were determined also for each transect ($P10$

$- P90$) along with all possible two-band ratios for the P values. The height percentile at

$P100$ equaled the range, the difference between the minimum point (bare earth) and the

maximum point (top of canopy). The relationship of species richness with a given

LIDAR-derived variable was determined by using scatterplots and simple linear regression, the resulting adjusted r^2 and standard error of the estimate (s) (SPSS Inc, Chicago, IL). This was repeated for all habitats combined and by habitat-type.

<div align="center">Results</div>

Species richness and habitats

Although 260 vascular plant species were reported previously for Horn Island (Eleuterius, 1979), only 69 species were found in the present study (Table 8). However, beach dunes were not sampled and our line-transect approach differed from earlier sampling methods. These factors may account for some portion of the apparent decline in Horn Island species richness over the past several decades.

Number of species per transect ranged from 0 to 12. At the lowest elevations, marsh habitat exhibited flooded to near-saturated soil with nearly 100 percent cover by vegetation and an average of only four species per transect dominated by black needle rush and saltmeadow cordgrass (Table 8). Woodlands were dominated by slash pine and also exhibited a high percent of vegetative cover and the greatest vegetation height per transect. In contrast, stable dunes on average included the greatest percentage of bare soil (sand) and were dominated by low shrub vegetation with a low species richness of four species per transect. Meadows and transition zones averaged approximately seven species per transect (Table 8). Meadows were characterized primarily by herbaceous vegetation dominated by torpedo grass and soils that varied from a wet peat covered by vegetation to exposed sand. Transition zones were located primarily between meadows and stable dunes and secondarily between marsh and stable dunes. Transition zone soils were often

moist and vegetation cover was 70 percent. This coverage was greater than in meadows and stable dunes but less than in woodlands and marshes.

Table 7. Field data of total number of species for each habitat and for all habitats combined along with species richness and cover with one standard deviation shown in parentheses. The 90 transect locations resulted in the following number of transects per habitat-type: meadow (16), stable dune (37), marsh (10), woodland (5), and transition zone (22). The last three columns were calculated from LIDAR data and represent the minimum (ground elevation), mean, and range (vegetation height) measured in meters for individual habitats and all habitats combined with one standard deviation shown in parentheses.

Habitat	Total Species	Species Richness	Cover (%)	Minimum	Mean	Range
Meadow	35	6.9 (3.0)	65 (30)	1.1 (0.2)	1.8 (0.7)	5.3 (5.1)
Stable Dune	32	4.4 (1.8)	58 (27)	1.7 (0.8)	3.4 (1.4)	7.0 (4.5)
Marsh	16	4.0 (1.4)	98 (6.0)	0.7 (0.2)	1.2 (0.4)	1.8 (0.8)
Woodland	12	4.8 (2.4)	86 (15)	1.0 (0.1)	5.6 (1.5)	16 (3.0)
Transition Zone	39	7.3 (2.1)	70 (23)	1.0 (0.3)	2.6 (1.5)	7.2 (5.1)
All Habitats Combined	69	5.6 (2.4)	68 (28)	1.3 (0.6)	2.8 (1.6)	6.7 (5.2)

Regression analyses

When data for all transects were combined ($n=90$), there were no significant relationships of richness per transect with any LIDAR index. However, within meadow, marsh, and woodland, significant ($p \leq 0.05$) relationships were found (Table 9).

A LIDAR-based signature for transects in each habitat can be visualized by graphing the height percentiles (Fig. 9.) The LIDAR signatures for marsh show that transects with higher species richness are associated with greater vegetation height as indicated by the strong correlation of species richness in marsh with the range ($P100$) (Fig. 9) as well as with $P90/P80$ (Table 9). The species-rich marsh transects all consisted not only of tall grass and grass-like marsh species but also shrubs including eastern baccharis, yaupon holly, and wax myrtle which contributed to the greater vegetation height. The mean height of returns also correlated significantly with species richness in marsh habitat (adjusted $r^2 = 0.36$, $s = 1.1$ species per transect).

LIDAR signatures for woodland transects indicated that greater species richness was associated with a more developed vegetation canopy (Fig. 9). Species richness regressed significantly with height at $P70$ (Fig.9, Table 9) and $P70/P90$. The woodland transect with the greatest richness had both a slash pine overstory and a dense yaupon holly and wax myrtle sub-canopy along with partial ground coverage by saltmeadow cordgrass about 1 m in height. The other transects were characterized by only a partial sub-canopy of shrubs and more bare soil exposure. The mean vertical distribution of points also correlated significantly with species richness in the woodland habitat (Table 9).

LIDAR signatures for meadow habitat were complex owing to a high variability in vegetation structure (Fig. 9). Meadow habitat consists of both low herbaceous vegetation along with some shrubs and occasional broadly-spaced slash pine. Overall species richness in meadow habitat was significantly related to $P70/P90$ (Table 9). In species-rich meadow transects, comprised of low herbaceous vegetation with sparsely-

distributed shrubs, a sharp increase in height between P70 and P90 was associated with an increase in richness. Meadow habitats with the fewest species were composed of vegetation that was similar in height with only a small increase in height between P70 and P90.

Table 8. Adjusted coefficient of determination (r^2), standard error of the estimate (s), and probability of a greater F statistic (Pr>F) from simple linear regressions of plant species richness per transect with vertical distribution descriptors, percentiles, and percentile ratios for Horn Island habitats.

Habitat	Index	Adjusted r^2	s	Pr > F
	Distribution Descriptor			
Marsh	Range	0.74	0.7	0.001
Woodland	Mean	0.91	0.7	0.008
	Percentile			
Woodland	P70	0.97	0.4	0.002
	Percentile Ratios			
Marsh	P90 / P80	0.41	1.0	0.03
Meadow	P70 / P90	0.27	2.5	0.02
Woodland	P70 / P90	0.85	0.9	0.02

Discussion and conclusions

When data for all habitat-types were combined, plant species richness did not correlate significantly with LIDAR-based indices. Also, plant species richness for stable dune and transition zone could not be estimated using any of the LIDAR metrics. However for marsh, meadow, and woodland considered individually, plant species richness could be estimated with precisions $\leq$ 2. 5 species per 15-m transect. No single index provided a best-fit estimation of richness among habitat-types.

Plant species richness in marsh habitat was significantly related to range (Fig 10), and the regression slope indicated that a greater richness was found where the vegetation was taller. To a lesser degree $P90/P80$ and the mean vertical distribution of returns correlated significantly with marsh species richness, signifying that richness is linked also with structural complexity of the vegetation canopy. Species-rich marsh habitat also consists of multi-layered vegetation such as shrubs; therefore, a slight increase in height between $P80$ and $P90$ is associated with greater species richness. While, sharp increases in height between $P80$ and $P90$ indicate lower species richness. Species-rich salt marsh habitats have been associated with both taller canopies and increased layering or structural complexity (Keer & Zedler, 2002). Also, species richness has been shown to increase with canopy height, three dimensional space-filling and greater biomass on grasslands (Spehn, Joshi, Schmid, Diemer, & Körner, 2000).

Height distribution percentiles determined from LIDAR data have provided accurate measurements of important stand characteristics such as tree height, basal area, timber volume, crown area, and biomass (Lim, Treitz, Wulder, St-Onge, & Flood, 2003; Means et al., 2000; Næsset, 2002). Also, the strong relationship between height

distribution and vertical structure of tree canopies has been used to evaluate understory features (Maltamo et al., 2005; Zimble et al., 2003). Multi-layered organization enhances structural complexity in forest canopies and increased vertical complexity is generally associated with high plant species diversity in forests (Bazzaz, 1975; Ishii, Tanabe, & Hiura, 2004). With respect to LIDAR data for woodland habitat, the best-fit regression for species richness was with canopy heights at the 70th percentile, where increased height indicates higher species richness (Fig. 9, 10). In addition, the height distribution ratio $P70/P90$, as well as the mean distribution of returns, was significantly related to richness in woodlands, indicating that increased structural complexity in woodland habitat correlated with a greater species richness. As with marsh, only slight increases in height between $P70$ and $P90$ were associated with greater species richness, whereas sharp increases were associated with low species richness.

Vegetation structure in meadow habitat showed more variability than in marsh or woodland and was characterized predominantly by low herbaceous vegetation and shrubs with occasional, sparse slash pine. Height and canopy cover of low vegetation has been estimated using LIDAR (Davenport, 2000; Streutker & Glenn, 2006; Weltz, Ritchie, & Dale Fox, 1994). In addition, Straatsma and Middelkoop 2007 found that the 95th percentile was best for predicting the height of low, herbaceous floodplain vegetation. $P70/P90$ regressed significantly with richness in meadow habitat (Fig 10). In contrast to woodland habitat, species richness in meadow increased with increasing height between $P70$ and $P90$ indicating that richness may increase with vegetation height, whereas structural complexity is less important.

The capability of LIDAR to accurately estimate vegetation height and structural complexity provides a promising means of detecting species richness. This study demonstrated plant species richness could be significantly estimated for meadow, marsh, and woodland habitats on Horn Island using vertical distribution descriptors and height percentiles of multiple-return airborne LIDAR. It is clear that habitat types must be addressed separately as species richness could not be accurately estimated for all habitats combined and there was no significant relationship for richness in stable dune or transition zone. Nonetheless, this study indicates a strong feasibility for utilizing LIDAR data alone to predict species richness on barrier islands.
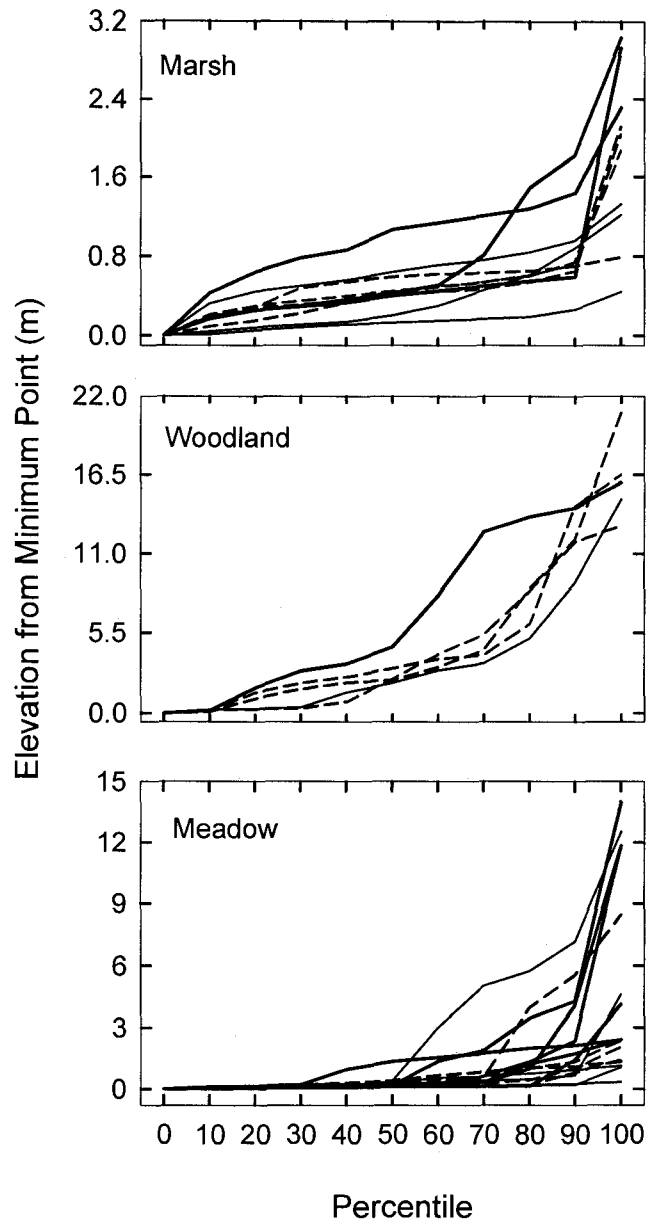
Fig. 9. LIDAR based signatures for marsh, woodland, and meadow transects produced by graphing height percentiles at each 10th percentile of height above the minimum. High (thick lines), moderate (dashed lines), and low (thin lines) species richness for each transect located within marsh (high ≥ 5, moderate $= 4$, low ≤ 3), woodland (high $= 9$, moderate $= 4$, low $= 3$), and meadow (high ≥ 9, moderate $\geq 5 \leq 8$, low ≤ 4)

Fig. 10. Regressions of plant species richness per transect with the index which produced

the greatest r^2 for a given habitat. The probability of a greater F was $p \leq 0.02$ for all

regressions shown.

CHAPTER V

SUMMARY

Vegetation patterns and species richness are functions of individual species reactions to abiotic and biotic conditions and extreme episodic events. In order to understand how plant composition and species richness will respond to climate change, increased storm frequency and anthropogenic pr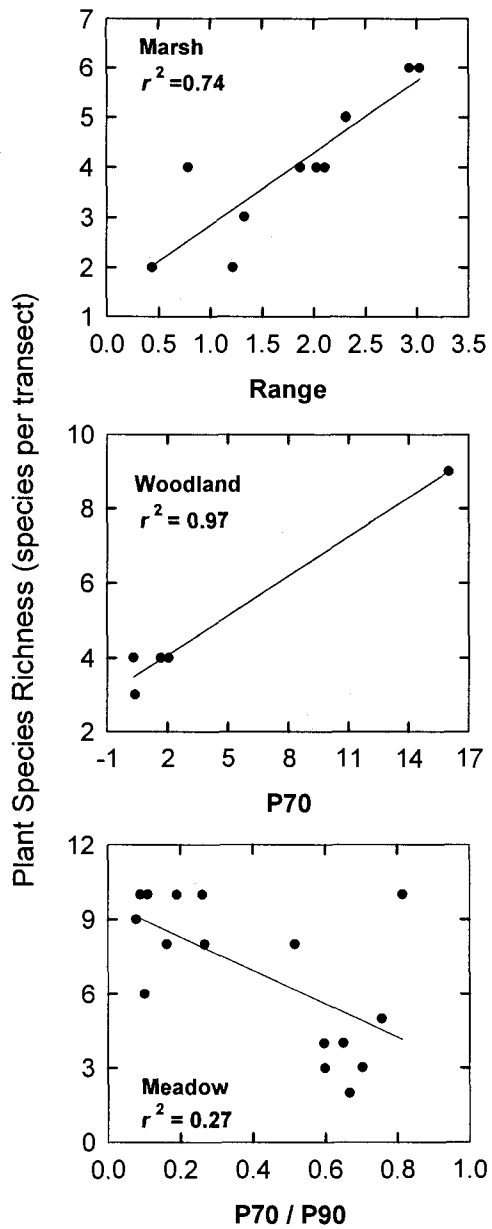essures, efficient and rapid methods of assessing and monitoring vegetation is necessary. Vegetation assessment through the use of remote sensing is becoming a powerful approach in evaluating species richness and monitoring change.

In Mississippi, Horn Island presents an ideal setting to develop remote sensing methods in coastal vegetation assessment because it is protected from development and relatively undisturbed by human activity; nonetheless, bordering the ocean, it is the first to be affected by relative sea-level rise. This study analyzed vegetation composition and plant species richness on Horn Island using ground measurements in conjunction with remotely sensed spectral and LIDAR data.

Chapter II analyzed and classified the vegetation composition on Horn Island. Results indicated that vegetation on Horn Island can be identified and classified based on indicator species that are consistent both over time and among other Gulf of Mexico barrier islands. Also, improving automatic classification accuracy of vegetation on Horn Island at fine spatial scales (3m) can be achieved by including multiple data types that provide heterogeneous information as indicated by the improved classification accuracy of the combined spectral and LIDAR data over hyperspectral or LIDAR data alone. In addition, despite uncertainties in the mapping techniques used for the 1979 vegetation

map, this study was able to make broad comparisons on vegetation changes and link some changes in vegetation to geomorphological changes on Horn Island.

Chapter III examined the relationships between measured plant species richness and remotely sensed spectral indices based on within-transect means or spatial variability. Results showed that habitat-types must be addressed separately and no single index provided a best-fit estimation of richness within individual habitat-types. A test of index fidelity, based on the consistency of index response to changes in plant and environmental moisture, was applied to each of the indices. Among the 7 indices found to be significant at estimating species richness, 2 responded to changes in water content, while 5 did not respond to changes in water content. These indices indicate that environmental moisture along with moisture in leaves and soil are important for estimating species richness in marsh, and LAI and biomass are important for estimating the number of species in woodland, meadow, and transition zone. The advantage of quantifying within-transect spatial variability in index value was demonstrated in the capability of R ratios to estimate richness for four of the five habitat-types.

Chapter IV examined the relationships between measured plant species richness and the vertical distribution of airborne multiple-return LIDAR. This study demonstrated plant species richness could be significantly estimated for meadow, marsh, and woodland habitats on Horn Island using vertical distribution descriptors and height percentiles of multiple-return LIDAR data. It is clear that habitat types must be addressed separately as species richness could not be accurately estimated for all habitats combined and there was no significant relationship for richness in stable dune or transition zone. Vegetation height was important for estimating plant species richness in marsh, meadow, and

woodlands, and increased structural complexity was also important for predicting plant species richness in marsh and woodland.

In conclusion, this study showed that classifying vegetation on Horn Island can be achieved by using known ground targets and remotely sensed spectral or LIDAR data acquired at high spatial resolution ($\leq$ 3 m). However, automatic classification using combined spectral and LIDAR data in conjunction with ground data provides a more accurate means to rapidly classify vegetation. Although some changes in vegetation can be evaluated by comparison with previous vegetation maps, uncertainties in mapping techniques may require classifying vegetation using the same protocols and mapping techniques for all data sources. This study also showed that utilizing remotely sensed data to estimate plant species richness offers a promising resource of rapidly assessing and monitoring plant biodiversity on barrier islands. A fine spectral and spatial resolution and use of near-to-mid infrared spectral bands were shown to be important in assessing plant species richness for Horn Island habitats indicating water content and moisture are an essential biophysical element in assessing plant species richness in marsh and biomass and LAI are important at estimating richness in woodland, meadow, and transition zone. In addition, the ability of LIDAR to accurately estimate vegetation height and structural complexity shows excellent potential in evaluating species richness as indicated by the relationships of plant species richness with vegetation height descriptors and height percentiles.

APPENDIX A

SPECIES LIST

The vascular plant species recorded from the 100 transects sampled during this study represented three divisions of plant life: Pteriodophyta, Coniferophyta, and Magnoliophyta. The species were divided into 26 families with Poaceae, Asteraceae, and Cyperaceae containing 25%, 10%, and 7%, respectively, of the total species. The 100 transect locations resulted in the following number of species per habitat-type: marsh (16), meadow (38), stable dune (34), transition zone (44), and woodland (12).

There was 5 unidentified species (2 located in meadow, 2 located in stable dune, and 1 located in woodland). The other 64 species are listed below.

Key to habitats:
MH - Marsh
MD - Meadow
SD – Stable Dune
TZ – Transition Zone
WD - Woodland

Division
      Family
            Species **(Habitat Locations)**
Pteridophyta
      Dennstaedtiaceae
            Pteridium aquilinum (L.) Kuhn **(SD)**
Coniferophyta
      Pinaceae
            Pinus elliottii Engelm. **(MD, SD, TZ, WD)**

Magnoliophyta (Dicots)
      Anacardiaceae
            Rhus copallinum L. **(MD, SD, TZ, WD)**
            Toxicodendron radicans (L.) Kuntze **(WD, TZ)**
      Apiaceae
            Centella asiatica (L.) Urb. **(MD, TZ)**
            Hydrocotyle bonariensis Comm. ex Lam **(MD, TZ)**
      Aquifoliaceae
            Ilex vomitoria Aiton **(MD, SD, TZ, WD)**

Asteraceae
    Baccharis halimifolia L **(MH, MD, TZ)**
    Balduina angustifolia (Pursh) B.L. Rob. **(SD, TZ)**
    Chrysoma pauciflosculosa (Michx.) Greene **(MD, SD, TZ)**
    Euthamia leptocephala (Torr. & A. Gray) Greene ex Porter & Britton **(MD, TZ)**
    Heterotheca subaxillaris (Lam.) Britton & Rusby **(MD, SD)**
    Iva frutescens L. **(TZ)**
    Mikania scandens (L.) Willd. **(MD)**
    Solidago sempervirens L **(MD)**
Brassicaceae
    Cakile constricta Rodman **(SD, TZ)**
Cactaceae
    Opuntia ficus-indica (L.) Mill **(MD, SD, TZ)**
    Opuntia humifusa (Raf.) Raf **(MD, SD, TZ)**
Caryophyllaceae
    Paronychia erecta (Chapm.) Shinners **(SD, TZ)**
    Stipulicida setacea Michx **(SD, TZ)**
Cistaceae
    Helianthemum arenicola Chapm. **(SD, TZ)**
    Lechea sessiliflora Raf. **(MD, SD, TZ)**
Convolvulaceae
    Ipomoea imperati (Vahl) Griseb. **(SD)**
    Ipomoea sagittata Poir. **(MH)**
Clusiaceae
    Hypericum gentianoides (L.) Britton, Sterns & Poggenb **(MD, TZ)**
    Hypericum hypericoides (L.) Crantz **(MD, TZ)**
Empetraceae
    Ceratiola ericoides Michx **(SD, TZ)**
Fabaceae
    Chamaecrista fasciculata (Michx.) Greene **(SD)**
Fagaceae
    Quercus geminata Small **(SD, WD)**
Malvaceae
    Hibiscus grandiflorus Michx. **(MH)**
Myricaceae
    Morella cerifera (L.) Small **(MH, MD, SD, TZ, WD)**
Onagraceae
    Ludwigia maritima Harper **(MH, MD, TZ)**
    Oenothera humifusa Nutt **(SD)**
Rosaceae
    Rubus trivialis Michx **(MH, MD, SD, TZ, WD)**
Rubiaceae
    Diodia teres Walter **(MD, TZ)**
Magnoliophyta (Monocots)
    Agavaceae

Yucca gloriosa L. **(SD)**

Arecaceae

Serenoa repens (Bartram) Small **(SD, TZ)**

Cyperaceae

Cladium mariscus (L.) Pohl ssp. *jamaicense* (Crantz) Kük. **(MH, TZ)**

Cyperus lecontei Torr. ex Steud. **(MD, SD, TZ)**

Eleocharis flavescens (Poir.) Urb. var. *flavescens* **(MD, TZ)**

Fimbristylis caroliniana (Lam.) Fernald **(MD)**

Juncaceae

Juncus megacephalus M.A. Curtis **(MD, TZ)**

Juncus roemerianus Scheele **(MH, MD, TZ)**

Juncus scirpoides Lam **(MD, TZ)**

Orchidaceae

Spiranthes praecox (Walter) S. Watson **(MD)**

Poaceae

Andropogon mohrii (Hack.) Hack. ex Vasey **(TZ)**

Andropogon virginicus L. **(MD, SD, TZ)**

Aristida purpurascens Poir. **(SD)**

Dichanthelium dichotomum (L.) Gould **(MD, SD, TZ)**

Distichlis spicata (L.) Greene **(MD, TZ)**

Panicum amarum Elliot var. *amarulum* (Hitchc. & Chase) P.G. Palmer **(TZ)**

Panicum repens L. **(MH, MD, SD, TZ, WD)**

Panicum virgatum L. **(MH, MD)**

Phragmites australis (Cav.) Trin. ex Steud. **(MH)**

Schizachyrium maritimum (Chapm.) Nash **(MD, SD, TZ)**

Setaria parviflora (Poir.) Kerguélen **(MH)**

Spartina alterniflora Loisel. **(MH)**

Spartina patens (Aiton) Muhl. **(MH, MD, TZ, WD)**

Sporobolus virginicus (L.) Kunth **(SD)**

Uniola paniculata L. **(SD, TZ)**

Smilacaceae

Smilax auriculata Walter **(SD, TZ, WD)**

Smilax bona-nox L. **(MH, MD, SD, TZ, WD)**

Typhaceae

Typha angustifolia L **(MH)**

Xyridaceae

*Xyris ambigua* Bey. ex Kunth **(MD, TZ)**

APPENDIX B

CLASSIFICATION MAPS

The ML classification results indicated that integration of LIDAR and HyMap data improved the overall classification accuracy over classifications of LIDAR or HyMap data alone for all categories except stable dune habitat. Stable dune did show improved accuracy for the combined data classification over HyMap by decreasing omission error although commission errors showed a slight increase. However, the overall accuracy for stable dune habitat classified from LIDAR was reduced when the combined data were classified. Shoreline and beach dune were misclassified as stable dune in the combined classification. Shoreline classification showed improved accuracy with decreased omission and commission errors for the combined classification over LIDAR or HyMap alone. Shoreline was often classified as beach dune in the HyMap classification and as marsh in the LIDAR classification. The most drastically improved classification accuracy was marsh habitat in the combined classification over the LIDAR classification. The omission and commission errors of each classification can be visualized in the following HyMap, LIDAR, and Combined vegetation maps.
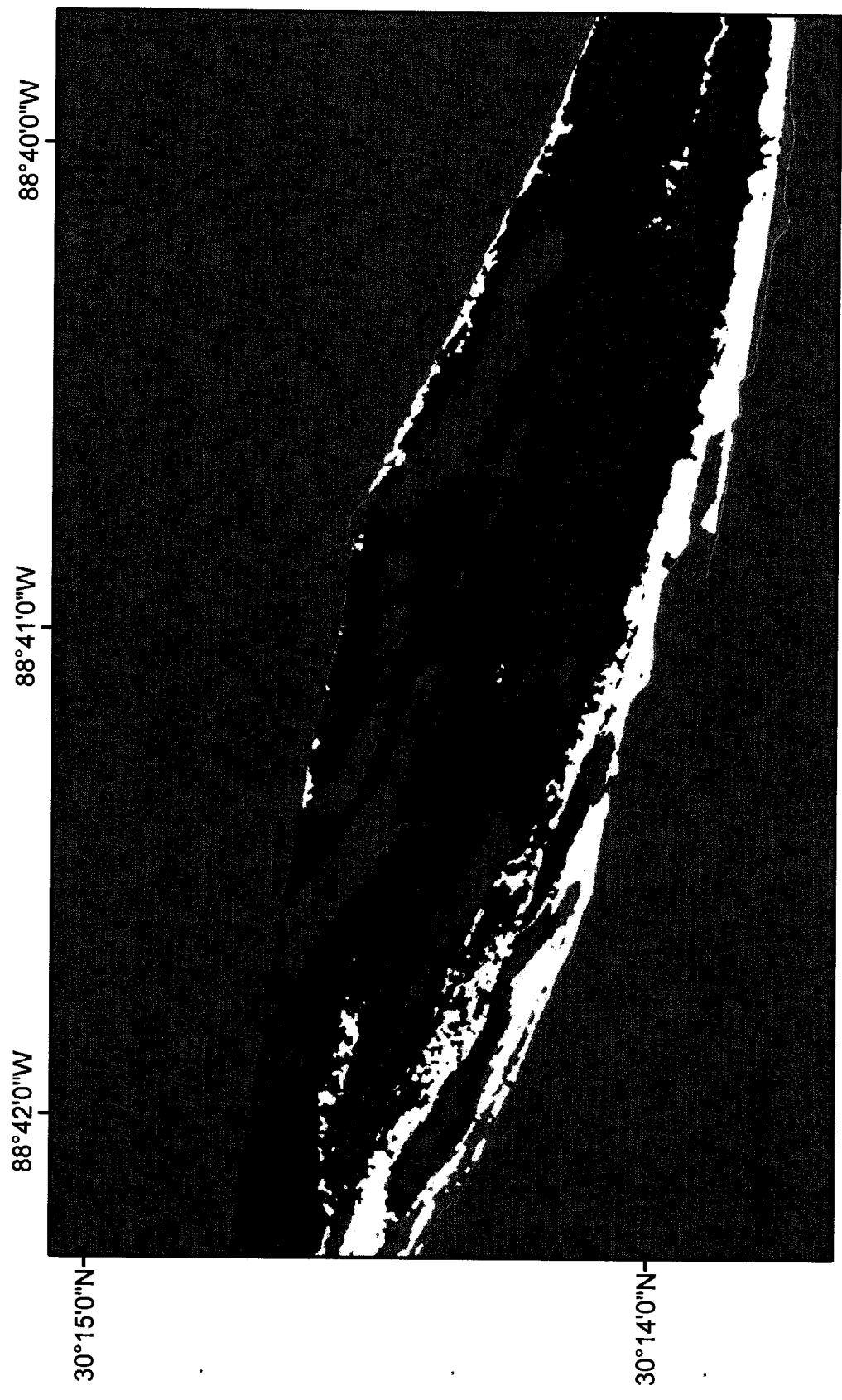
Legend

SHORELINE

MEADOW

WATER

BEACH DUNE

MARSH

STABLE DUNE

WOODLAND

The above legend applies to the maps that follow.
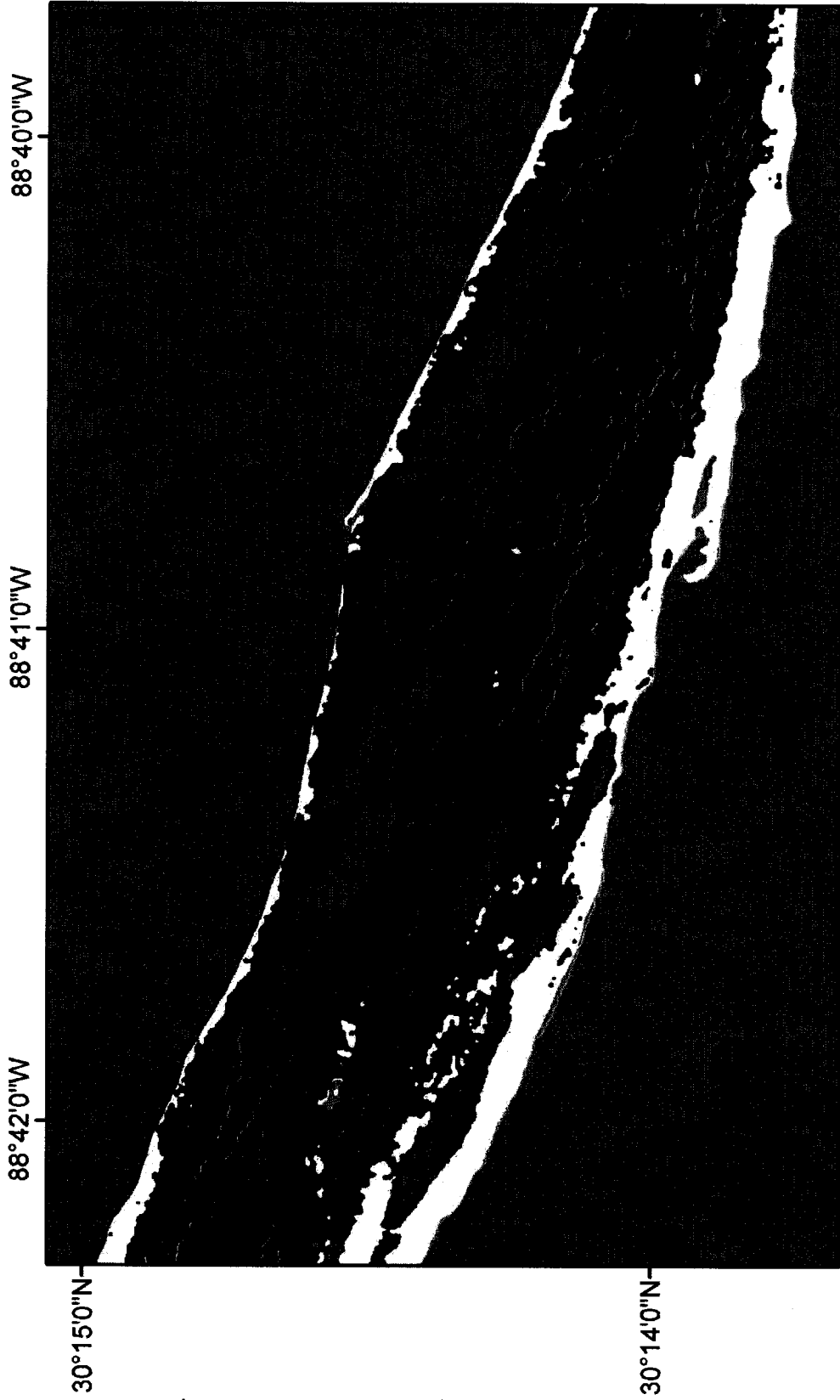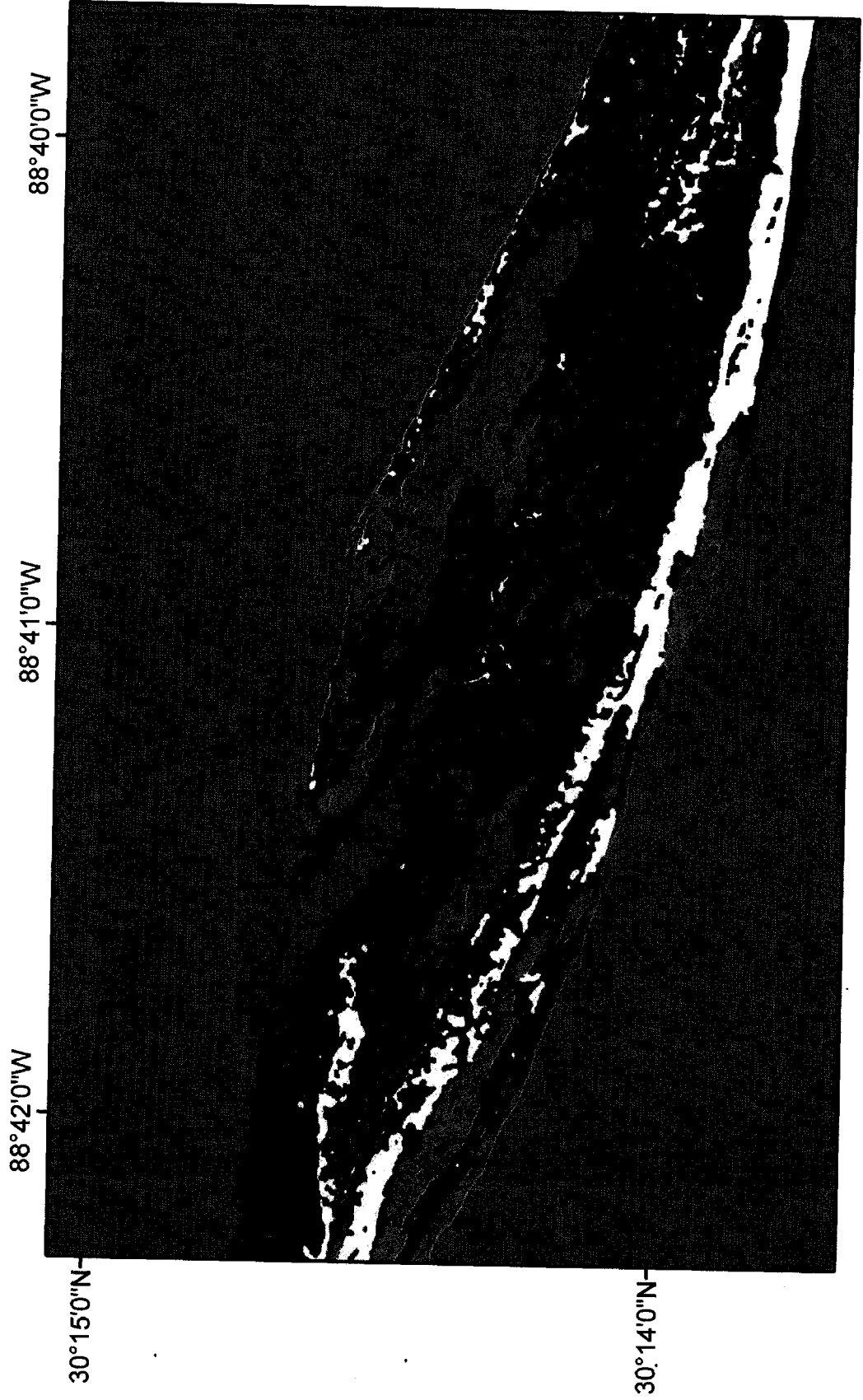
REFERENCES

Acosta, A., Carranza, M.L. & Izzi, C.F. (2005). Combining land cover mapping of
coastal dunes with vegetation analysis. *Applied Vegetation Science*, 8, 133-138.

Asner, G.P. (1998). Biophysical and biochemical sources of variability in canopy
reflectance *Remote Sensing of the Environment*. 64, 234-253.

Bachmann, C.M., Donato, T.F., Lamela, G.M., Rhea, W. J., Bettenhausen, M.H., Fusina,
R.A.,et al., (2002). Automatic classification of land cover on Smith Island, VA, using
HyMap imagery. *IEEE Transactions on Geoscience and Remote Sensing*, 40, 2313-
2330.

Barbour, M. G., Davis, M. R., Johnson, A.F., & Pavlik, B.M. (1987). Beach vegetation
and plant distribution patterns along the northern Gulf of Mexico. *Phytocoenologia*,
15, 201-233.

Bazzaz, F. A. (1975). Plant species diversity in old-field successional ecosystems in
southern Illinois. *Ecology*, 56, 485-488.

Burkhalter, J.R. (1987). An ecological study of coastal strand vegetation on the western
end of Santa Rosa Island near Pensacola, Florida. (Masters Thesis, University of
West Pensacola, 1987). Pensacola, Florida. 195.

Byrnes, M.R., McBride, R.A., Penland, S., Hiland, M.W., & Westphal, K.A. (1991).
Historical changes in shoreline position along the Mississippi Sound barrier islands
GCSSEPM Foundation 12th Annual Research Conference, December 5, 1991.
Program and Abstracts pp. 43-55.

Carter, G. A. (1991). Primary and secondary effects of water content on the spectral
reflectance of leaves. *American Journal of Botany*, 78, 916-924.

Carter, G. A., Knapp, A. K., Anderson, J. E., Hoch, G. A., & Smith, M. D. (2005). Indicators of plant species richness in AVIRIS spectra of a mesic grassland. *Remote Sensing of the Environment* 98, 304-316.

Chapin, S. F. III, Zavaleta, E. S., Eviner, V. T., Naylor, R. L., Vitousek, P. M., Reynolds, H. L., et al. (2000). Consequences of changing biodiversity. *Nature*, 405, 234-242

Cipriani, L. E. & G. W. Stone. (2001). Net longshore sediment transport and textural changes in beach sediments along the Southwest Alabama and Mississippi barrier islands, U.S.A. *Journal of Coastal Research*, 17, 443-458.

Clark, M.L., Roberts, D. A. & Clark, D. B. (2005). Hyperspectral discrimination of tropical rain forest tree species at leaf to crown scales. *Remote Sensing of Environment*, 96, 375-398.

Craig, N.J, Turner, R.E., & Day, J.W. (1979). Land loss in coastal Louisiana (USA). *Environmental Management*, 3, 133-145.

Davenport, I.H., Bradbury, R.B., Anderson, G.R.F., Hayman, J.R., Krebs, J.R., Mason, D.C., et al. (2000). Improving bird population models using airborne remote sensing. *International Journal of Remote Sensing*, 21, 2705-2717.

Debinski, D. M., Kindscher, K.,& Jakubauskas, M. E. (1999). A remote sensing and GIS-based model of habitats and biodiversity in the Greater Yellowstone Ecosystem. *International Journal of Remote Sensing*, 20, 3281-3291.

Deramus, R. (1970). Studies on the flora of the vascular plants of Dauphin Island, (Doctoral dissertation, University of Alabama, Mobile County, Alabama, 74.

Doing, H. (1985). Coastal fore-dune zonation and succession in various parts of the world. *Vegatatio*, 61, 65-75.

Dorp, D. van der and Boot, R, & Maarel, E. van der. (1985). Vegetation succession on the dunes near Oostvoorne, the Netherlands, since 1934, interpreted from air photographs and vegetation maps. *Vegetatio*, 58, 123-136.

Douglass. S. L. (1994). Beach erosion and depositon on Dauphin Island, Alabama, USA. *Journal of Coastal Research*, 10, 306-328.

Downing, H G; Carter, G. A., Holladay, K. W., Cibula, W. G. (1993). The radiative-equivalent water thickness of leaves. *Remote Sensing of Environment*. 46, 103-107.

Dubayah, R.O., & Drake, J.B. (2000). Lidar remote sensing for forestry. *Journal of Forestry*, 98, 44-46.

Ehrenfeld, Joan G. (1990). Dynamics and processes of barrier island vegetation. *Reviews in Aquatic Sciences*, 2, 437-480.

Eleuterius, L.N. (1979). *A Phytosociological Study of Horn and Petit Bois Islands, Mississippi*. Coastal Field Research Laboratory, Southeast Regional Office, National Park Service, Final report, 192.

Gao, B.C., Heidebrecht, K.B., & Goetz, A.F.H. (1992). Atmospheric REMoval Program (ATREM) User's Guide, Center for the Study of Earth From Space document, University of Colorado, version 1.1, 24.

Gao, J., (1999). A comparative study on spatial and spectral resolutions of satellite data in mapping mangrove forest. *International Journal of Remote Sensing*, 20, 2823-2833.

Garcia, L.V., Marañón, T., Moreno, A. and Clemente, L. (1993). Above-Ground Biomass and Species Richness in a Mediterranean Salt Marsh. *Journal of Vegetation Science*, 4, 417-424.

Geevan, C.P. (1995). Biodiversity conservation information network: a concept plant. *Current Science*, 69, 906-914.

Genc, L., Dewitt, B., & Smith, S. (2004). Determination of wetland vegetation height with lidar. *Turkish Journal of Agriculture and Forestry,* 28, 63-71.

Genc, L., Smith, S.E.,& Dewitt, B.A. (2005). Using satellite imagery and LIDAR data to corroborate an adjudicated ordinary high water line. *International Journal of Remote Sensing,* 26, 3683-3693.

Gibson, D.J., & Looney, P.B. (1992). Seasonal variation in vegetation classification on Perdido Key, a Barrier Island off the Coast of the Florida, Panhandle, *Journal of Coastal Research,* 8, 943-955.

Godfrey P.J. (1976). Barrier Beaches of the East Coast. *Oceanus*, 19, 27-40.

Goetz, S., Steinberg, D., Dubayah, R.,& Blair, B. (2007). Laser remote sensing of canopy habitat heterogeneity as a predictor of bird species richness in an eastern temperate forest, USA. *Remote Sensing of Environment.* 108, 254-263.

Gong, P., Pu, R.L., and Yu, B. (1997). Conifer species recognition an exploratory analysis of in -situ hyperspectral data. *Remote Sensing of Environment*, 25, 707-715

Gornitz, V. (1995). Sea-level rise: A review of recent past and near-future trends, *Earth Surface Processes and Landforms,* 20, 7-20.

Gould, W. (2000). Remote Sensing of Vegetation, plant species richness, and regional biodiversity. *Ecological Applications*, 10, 1861-1870.

Griffith, J.A., Stehman, S.V., Sohn, T.L., & Loveland, T.R. (2000). Detecting trends in landscape pattern metrics over a 20-year period using a sampling-based monitoring programme. *International Journal of Remote Sensing*, 24, 75-181.

Hale, G. M., and Querry, M. R. (1973). Optical constants of water in the 200-nm to 200-micrometer wavelength region. *Applied Optics*, 12, 555-563.

Hayden B.P. & Hayden, N.R. (2003). Decadal and century-long storminess changes at long term ecological research sites. Greenland D., D.G. Goodin, R.C. Smith (Eds.), In *Climate variability and ecosystem climate variability and response at long-term ecological research sites* (262-285). New York: Oxford University Press.

Hayden, B.P., Santos, M. C.F.V., Shao, G., & Kochel, R.C. (1995). Geomorphological controls on coastal vegetation at the Virginia Coast Reserve. *Geomorphology*. 13, 283-300.

Hill, R.A., & Thomson, A.G. (2005). Mapping woodland species composition and structure using airborne spectral and LiDAR data. *International Journal of Remote Sensing*, 26, 2763-3779.

Holgate, S.J. & Woodworth, P.L. (2004). Evidence for enhanced sea level rise during the 1990s. *Geophysical Research Letters*, 31, L073.

Hooper, D. U. & Vitousek, P. M. (1997) The effects of plant composition and diversity on Ecosystem processes. *Science*, 277, 1302-1305.

Ishii, H.T., Tanabe, S. & Hiura, T. (2004). Exploring the relationship among canopy structure, stand productivity, and biodiversity of temperate forest ecosystems. *Forest Science*, 50, 342-355.

Janssen, J.A.M. (2004). The use of sequential vegetation maps for monitoring in coastal areas, *Community Ecology*, 5, 31-43.

Jensen, J. (2005). *Introductory Digital Image Processing. A Remote Sensing Perspective.* Upper Saddle River, NJ: Prentice Hall. p. 592.

Jorgensen, A. F. & Nohr H. (1996). The use of Satellite images for mapping of landscape and biological diversity in the Sahel. *International Journal of Remote Sensing*, 17, 91-109.

Kalacska, M., Sanchez-Azofeifa, G. A., Rivard, B., Caelli, T., White, P.H., & Calvo-Alvarado, J.C. (2007). Ecological fingerprinting of ecosystem succession: Estimating secondary tropical dry forest structure and diversity using imaging spectroscopy. *Remote Sensing of Environment*, 108, 82-96.

Kareiva, P.M. (1993). No shortcuts in new maps. *Nature,* 365, 292-293.

Keer, G.H. & Zedler, J.B. (2002). Salt marsh canopy architecture differs with the number and composition of species. *Ecological Applications*, 12, 456-473.

Kerr, J. T., Southwood, T. R. E. & Cihlar, J. (2001). Remotely sensed habitat diversity predicts butterfly species richness and community similarity in Canada. *Proceedings of the National Academy of Sciences*, 98, 11365-11370.

Knops, J.M. H., Tilman, D., Haddad, N., Naeem, S., Mitchell, C., Haarstad, J. et al. (1999). Effects of plant species richness on invasion dynamics, disease outbreaks, insect abundances and diversity. *Ecology Letters,* 2, 286-293.

LaRocque, P. E., Banic, J.R., & Cunningham, A.G. (2004). Design description and field testing of the SHOALS-1000T airborne bathymeter. Proc SPIE vol. 5412, Laser Radar Technology and Applications IX; Gary W. Kamerman, ed., pp. 162-1874.

Lauver, C. L. (1997). Mapping species diversity patterns in the Kansas shortgrass region by integrating remote sensing and vegetation analysis. *Journal of Vegetation Science*, 8, 387-394.

Lee, J.A. & Ignaciuk, R. (1985). The physiological ecology of strandline plants. *Plant Ecology, 62,* 319-326.

Lee, D.S., & Shan, J. (2003). Combining Lidar elevation data and IKONOS multispectral imagery for coastal classification mapping. *Marine Geodesy,* 26, 117-127.

Lefsky, M.A., Cohen, W.B., Acker, S.A., Spies, T.A., Parker, G.G., Harding D. (1999). Lidar remote sensing of biophysical properties and canopy structure of forest of Douglas-fir and western hemlock. *Remote Sensing of Environment, 70,* 339-361.

Lefsky, M. A., Cohen, W.B., Parker, G.G. & Harding, D.J. (2002). Lidar remote sensing for ecosystems studies. *BioScience,* 52, 19-30.

Lim, K., Treitz, P., Wulder, M., St-Onge, B.,& Flood., M. (2003). LiDAR remote sensing of forest structure. *Progress in Physical Geography, 27,* 55-106.

Looney, P. B., Gibson, D.J., Blyth, A., & Cousens, M.I. (1993). Flora of the Gulf Islands National Seashore, Perdido Key, Florida. Bulletin of the Torrey Botanical Club 120, 327-341.

Lucas, N.S., Shanmugam, S., & Barnsley, M. (2002). Sub-pixel habitat mapping of a coastal dune ecosystem. *Applied Geography.* 22, 253-270.

MacArthur, R.H.& MacArthur, J.W.1(1961). On bird species diversity. *Ecology,* 42, 594-598.

Maltamo, M. Packalén, P.Yu, X., Eerikäinen, Hyyppä, J., & Pitkänen, J. (2005). Identifying and quantifying structural characteristics of heterogeneous boreal forest using laser scanner data. *Forest Ecology and Management,* 216, 41-50.

Means, J. E., Scker, S. A., Fitt, B.J., Renslow, M., Emverson, L. & Hendrix, C. J. (2000). Predicting forest stand characteristics with airborne scanning lidar. *Photogrammetric Engineering and Remote Sensing*, 66, 1367-1371.

Miller, G.J., & Jones, S.B. Jr. (1967). The vascular flora of Ship Island, Mississippi. *Castane,*. 32, 84-89.

Mooney, H.A.& Chapin, F.S.III. (1994). Future directions of global change research in terrestrial ecosystems. *Trends in Ecology and Evolution,* 9, 371-372.

Moore, F.R., Kerlinger, P., & Simons, T. R. (1990). Stopover on a gulf coast barrier island by spring trans-gulf migrants. *Wilson Bulletin*, 102, 487-500.

Moreno-Casasola, P., & Espejel, H. (1986). Classification and ordination of coastal sand dune vegetation along the Gulf and Caribbean Sea of Mexico. *Vegetatio,* 66, 147-182.

Næsset E. (2002). Predicting forest stand characteristics with airborne scanning laser using a practical two-stage procedure and field data, *Remote Sensing of Environment*, 80, 88-99.

Naeem, S., Thompson, L.J., Lawler, S.P., Lawton, J.H., & Woodfin, R.M. (1995). Empirical evidence that declining species diversity may alter performance of terrestrial ecosystems. *Philosophical Transactions: Biological Sciences*, 347, 249-262.

Nagendra, H. (2001). Using remote sensing to assess biodiversity. *International Journal of Remote Sensing*, 22, 2377-2400.

Nagendra, H.& Gadgil, M. (1999). Satellite Imagery as a tool for monitoring species diversity: an assessment. *Journal of Applied Ecology*, 36, 388-397.

Nayegandhi, A., Brock, J.C., Wright, C.W., & O'Connell, M.J. (2006). Evaluating a

small footprint, waveform-resolving lidar over coastal vegetation communities.

Photogrammetric Engineering and Remote Sensing, 72, 1407-1417.

Nelson, R., Oderwald, R., & Gregoire, T.G. (1997). Separating the ground and airborne

laser sampling phases to estimate tropical forest baseal area, volume, and biomass.

Remote Sensing of Environment, 60, 311-326.

Oindo, B. O., Skidmore, A. K., & De Salvo, P. (2003). Mapping habitat and biological

diversity in the Massai Mara ecosystem. *International Journal of Remote Sensing*, 24,

1053- 1069.

O'Neill, R. V., Hunsaker, C. T., Jones, B., Ritters, K. H., Wickham, J. D., Schwartz, P.

M., et al. (1997). Monitoring environmental quality at the landscape scale.

BioScience, 47, 513-519.

Oosting, H. J. (1954). Tolerance to salt spray of plant of coastal dunes. *Ecology*, 26, 85-

89.

Otvos, E.G. (1970). Development and migration of barrier islands, northern Gulf of

Mexico. *Geological Society of America Bulletin.* 81, 241-246.

Otvos, E.G. (1979). Barrier island evolution and history of migration, north central Gulf

Coast. In SP Leatherman (Ed) *Barrier islands from the Gulf of St. Lawrence to the

Gulf of Mexico* (291-320). Academic Press, NY.

Otvos, E. G., & Carter, G.A. (2008). Hurricane degradation – barrier development cycles,

northeastern Gulf of Mexico: landform evolution and island chain history. *Journal of

Coastal Research*, in press.

Penfound, W.T. & O'Neill, M.E. (1934). The vegetationof Cat Island, Mississippi.

Ecology, 15, 1-16.

Penuelas, J., Pinol, J., Ogaya, R., & Filella, I. (1997). Estimation of plant water

concentration by the reflectance Water Index WI (R900/R970). *International Journal*

of Remote Sensing, 18, 2869-2875.

Pessin, L.J., & Burleigh, T.D. (1942). Notes on the forest biology of Horn Island,

Mississippi. *Ecology*, 22, 70-78

Pilkey, O.H. (2003). *A Celebration of the World's Barrier Islands*.. New York: Columbia

University Press.

Raber, G. T., Jensen, J.R., Schill, S.R., & Schuckman, K. (2002). Creation of digital

terrain models using an adaptive lidar vegetation point removal process.

Photogrammetric Engineering and Remote Sensing, 68, 1307-1315.

Ramsey, E.W. III., Nelson, G.A., Echols, D., & Sapkota, S.K. (2002). The national

vegetation classification standard applied to the remote sensing classification of two

semiarid environments. *Environmental Management*, 29, 703-715.

Rey-Benayas, J. M. & Pope, K. O. (1995). Landscape ecology and diversity patterns in

the seasonal tropics from Landsat TM imagery. *Ecological Applications*, 5, 386-394.

Rheinhardt, R.D., & Faser, K. (2001). Relationship between hydrology and zonation of

freshwater swale wetlands on lower Hatteras Island, North Carolina, USA, *Wetlands*,

21, 265-273.

Riffel, S.K., Keas, B.E., & Burton, T.M. (2001). Area habitat relationships of birds in

Great Lakes coastal wet meadows. *Wetlands*, 21, 492-507.

Seto, K. C., Fleishman, E., Fay, J. P. ,& Betrus, C. J. (2004). Linking spatial patterns of

bird and butterfly species richness with Landsat TM derived NDVI. *International*

Journal of Remote Sensing, 25, 4309-4324.

Shinkle, K.D., & Dokka, R.K. (2004). Rates of vertical displacement at benchmarks in the lower Mississippi Valley and the northern Gulf Coast. NOAA Technical Report, NOS/NGS 50, 135

Shao, G., Shugart, H. H.,& Hayden, B. P. (1996). Functional Classifications of Coastal Barrier Island Vegetation. *Journal of Vegetation Science*, 7, 391-396.

Snyder, R. A. & Boss, C. L. (2002). Recovery and Stability in Barrier Island Plant Communities. *Journal of Coastal Research*, 18, 530-536.

Spehn, E.M., Joshi, J., Schmid, B., Diemer, M., & Körner, C. (2000). Above-ground resource use increases with plant species richness in experimental grassland ecosystems. *Functional Ecology*, 14, 326-337.

Stauble, D.K. (1989). Barrier islands: Process and Management. Coastal Zone'89 the Sixth Symposium on Coastal and Ocean management held in Charleston, South Carolina, July 11- 14, 1989.

Stive, M.J.F.& Hammer-Klose, E.S. (2004). How important is global warming for coastal erosion? *Climatic Change*, 64, 27-39.

Stohlgren, T. J., Coughenour, M. B., Chong, G. W., Binkley, D., Kalkhan, M., Schell, L. D. et al. (1997). Landscape analysis of plant diversity. *Landscape Ecology*, 12, 155-170.

Stoms, D. M. & Estes, J. E. (1993). A remote sensing research agenda for mapping and monitoring biodiversity. *International Journal of Remote Sensing*, 14, 1839-1860.

Stoms, D.M. (1994). Scale dependence of species richness maps. *Professional Geographer*, 46, 346-358.

Straatsma, M., & Middelkoop, H. (2006). Extracting structural characteristics of

herbaceous floodplain vegetation under leaf-off conditions using airborne laser

scanner data. *International Journal of Remote Sensing*, 28, 2447-2467.

Streutker, D. R. & Glenn, N.F., (2006). LiDAR measurements of sagebrush steepe

vegetation heights. Remote Sensing of Environment, 102, 135-145.

Tews, J., Drose, U., Grimm, V., Tielbörger, Wichmann, M.C., Schwager, M. et al.

(2004). Animal species diversity driven by habitat heterogeneity/diversity: the

importance of keystone structures. *Journal of Biogeography*, 31, 79-92.

Thenkabail, P.S., Hall, J., Lin, T., Ashton, M.S., Haris, D., & Enclona, E.A. (2003).

Detecting floristic structure and pattern across topographic and moisture gradients in

a mixed species Central African forest using IKONOS and Landsat-7 ETM+ images.

International Journal of Applied Earth Observation and Geoinformation, 4, 255-270.

Thenkabail, P. S., Enclona, E. A., Ashton, M. S., & Van Der Meer, B. (2004). Accuracy

assessments of hyperspectral waveband performance for vegetation analysis

applications. *Remote Sensing of the Environment*, 91, 354-376.

Tilman, D., Knops, J., Wedin, D., Reich, P., Ritchies, M., & Siemann, E. (1997). The

influence of functional diversity and composition on ecosystem processes. *Science*,

277, 1300-1302.

Tsai, F. and Philpot, W. (1998). Derivative Analysis of Hyperspectral Data. *Remote

Sensing of Environment*, 66: 41-51.

Turner, W., Spector, S., Gardiner, N., Fladeland, M., Sterling, E., & Steininger, M.

(2003). Remote sensing for biodiversity science and conservation. *Trends in Ecology

and Evolution*, 8, 306-314.

USCOP (US Commission on Ocean Policy). (2004). *An Ocean Blueprint for the 21st*

Century. Washington, DC: US Commission on Ocean Policy. Final report.

Van Aardt, J.A.N., & Wynne, R.H. (2001). Spectral separability among six southern tree species *Photogrammetric Engineering and Remote Sensing* 67, 1367-1375

Wang, Y., Traber, M., Milstead, B., & Stevens, S. (2007). Terrestrial and submerged aquatic vegetation mapping in Fire Island National Seashore using high spatial resolution remote sensing data. *Marine Geodesy*, 30, 77-95.

Weltz, M. A., Ritchie, J.C. & Dale Fox, H. (1994). Comparison of laser and field measurements of vegetation height and canopy cover. *Water Resource Research*, 30, 1311-1319.

Williams, S.E., Marsh, H. & Winter, J. (2002). Spatial scale, species diversity, and habitat structure: Small mammals in Australian tropical rain forest. *Ecology*, 82, 1317-1329.

Zhang, J., Rivard, B., Sanchez-Azofeifa, A., & Castro-Esau, K. (2006). Intra- and inter-class spectral variability of tropical tree species at La Selva, Costa Rica: Implications for species identification using HYDICE imagery. *Remote Sensing of Environment*, 105, 129-141.

Zhang, K., Douglas, B.C., & Leatherman, S.P., (2004). Global warming and coastal erosion. *Climatic Change*, 64, 41-58.

Zimble, D.A., Evans, D.L., Carlson, G. C., Parker, R. C., Grado, S. C., & Gerard, P. D., (2003). Characterizing vertical forest structure using small-footprint airborne LiDAR. *Remote Sensing of Environment*, 87, 171-182.